THE PENNSYLVANIA STATE UNIVERSITY
SCHREYER HONORS COLLEGE

DEPARTMENT OF MATERIALS SCIENCE AND ENGINEERING

Rheology of Native Cellulose in Ionic Liquid/DMSO Solutions

VICTORIA BELKA
SPRING 2022

A thesis
submitted in partial fulfillment
of the requirements
for a baccalaureate degree
in Materials Science
with honors in Materials Science

Reviewed and approved* by the following:

Ralph Colby
Professor of Materials Science and Engineering and Chemical Engineering
Thesis Supervisor

Robert Kimel
Associate Teaching Professor of Materials Science and Engineering
Honors Adviser

* Electronic approvals are on file.

ABSTRACT

As the world seeks to decrease its reliance on synthetic polymers, many have looked to cellulose as the future of textiles, fibers, and consumer products. Cellulose is the most abundant biopolymer on Earth, and is currently used in the manufacturing of a variety of materials and products. The biopolymer's low cost, biocompatibility, and biodegradable nature have made it an attractive substitute for petroleum-based plastics in industries ranging from construction to cosmetics. However, the widespread usage of cellulose is severely restricted by its resistance to traditional methods of processing and dissolution. The extremely strong network of inter- and intramolecular hydrogen bonds in cellulose requires the use of toxic, volatile chemicals and expensive, energy-intensive processing methods. Since 2002, ionic liquids (ILs) have garnered interest as an alternative solvent for cellulose due to their nonvolatile, nontoxic, and non-derivatizing nature. Though ionic liquids such as 1-ethyl-3-methylimidazolium acetate (EMImAC) have been shown to effectively dissolve cellulose, the high viscosities of the resultant cellulose/IL systems have also limited their use in industry. Recent literature has suggested that a potential solution involves the addition of a cosolvent molecule like dimethyl sulfoxide (DMSO), which acts to further solvate the cations in the ionic liquid to increase the availability of the anions, the main agent responsible in cellulose dissolution.

This thesis investigates the effect of adding the cosolvent DMSO to cellulose/IL solutions by evaluating and comparing the rheological behavior of solutions of varying concentrations of cellulose in either 100% EMImAC or 50% EMImAC and 50% DMSO. The intrinsic viscosities of samples with concentrations of 0.05wt%, 0.1wt%, 0.2wt%, and 0.3wt% cellulose in both solvent mixtures were calculated through capillary viscometry and the creation of a Huggins and

Kraemer plot at 20°C and 80°C. The solutions containing DMSO were found to be less viscous than the solutions without DMSO, and it was determined that the quality of DMSO as a cellulose solvent increased with temperature. Additionally, the complex viscosity, loss modulus, and storage modulus of each sample were measured through interfacial rheology. The frequency sweeps of the solutions containing DMSO were found to have complex viscosities several orders of magnitude smaller than that of the 100% EMImAC solutions of the same concentration of cellulose. Ultimately, the conclusion that the addition of a cosolvent such as DMSO could increase the processability of cellulose/ionic liquid solutions by lowering the viscosity of the system was supported by the results of this study. These results may promote sustainability by reducing the reliance on nonrenewable resources such as petroleum through increasing the viability of biodegradable, sustainable systems like cellulose/ionic liquid solutions.

TABLE OF CONTENTS

LIST OF FIGURES

LIST OF TABLES

ACKNOWLEDGEMENTS

I would first like to acknowledge Dr. Ralph Colby for welcoming me into the wonderful world of rheology, and for encouraging me to explore my interest in cellulose and fiber-spinning. My experience in his research group has been instrumental in helping me grow as a scientist and a student, and has inspired me to pursue graduate research before starting my career in industry. This project would not have been completed without the guidance of Aijie Han, who went above and beyond her role to prepare me for laboratory research and troubleshoot the complications that arose during this study. I am also incredibly grateful for the help and support of Dr. Daniele Parisi and Josh Bostwick, who continued to aid my research even after they left Penn State. As I continue my research at the graduate level, I hope to be as instructive, patient, and helpful as my mentors in the Colby lab have been to me. I want to thank all of the current and former members of the Colby lab that I worked with during my time here, and I wish you all good luck in continuing your research and studies.

To my sister Elizabeth, who supported me despite pursuing her own education and listened to me describe my research again and again: I cannot possibly thank you enough. I am also incredibly grateful for the guidance, support, and endless proofreading provided by my parents, Angel and George Belka, without whom I would never have been able to pursue this degree. Finally, I would like to thank my family and friends, who supported me wholeheartedly throughout my time at Penn State despite never really knowing what materials science is.

Chapter 1

Introduction

As the demand for renewable and biodegradable products rises, cellulose has become an attractive substitute to petroleum-based plastics due to its abundance, low cost, biocompatibility, and biodegradability [1]. Cellulose, the most abundant biopolymer on earth, is currently used in the textile industry, construction, and for various consumer goods. Generally cellulose must be dissolved in order to be processed, but conventional solvents utilized in industry give rise to serious complications, such as volatility, toxicity, high cost, difficulty in solvent recovery, high processing temperature, and process instability [2]. Since 2002, research has focused on the use of ionic liquids (ILs) as alternative solvents for cellulose due to their nontoxic, nonvolatile nature. Though ionic liquid solvents eliminate some of the problems associated with traditional solvents, slow dissolution rates, high dissolution temperatures, and high viscosity of the solutions still prohibit the wide scale application of ionic liquids in cellulose processing [2]. Recent research has suggested that the inclusion of a cosolvent molecule in the cellulose/IL system dramatically reduces the viscosity, dissolution rate, and dissolution temperatures [3]. This paper discusses the current literature on cellulose dissolution in ionic liquids and studies the effect of adding the cosolvent dimethyl sulfoxide (DMSO) to solutions of cellulose and the ionic liquid 1-ethyl-3-methylimidazolium acetate.

Cellulose

Cellulose is a biopolymer found in the structural components of plants, fungi, green algae, and the outer membrane of certain marine animals [4]. The cellulose in plants is usually combined with hemicellulose and lignin, with the cellulose content varying by source. Cotton, the source of the cellulose studied in this paper, is approximately 90 wt% cellulose [4]. Cellulose is a homopolymer of anhydroglucose formed from repeating D-glucopyranose ring units linked by β-1,4-glycosidic bonds [5]. The reactive hydroxyl groups on each ring, the glycosidic linkages, and the oxygen atoms form inter- and intramolecular hydrogen bonds, which greatly influence the properties and dissolution behavior of cellulose [4]. The chemical structure of cellulose, as well as the system of intermolecular and intramolecular hydrogen bonds, is depicted in figure 1 [6]. The intramolecular hydrogen bonds are responsible for the high rigidity and chain stiffness of the molecules, which causes cellulose to form highly viscous solutions compared to polysaccharides like starch or dextran [7]. The high chain stiffness also increases the tendency to crystallize and encourages the formation of fibrillar assemblies [7]. The system of intermolecular bonds between cellulose chains causes the strong interactions between cellulose chains [4]. In order to dissolve and process cellulose, both the inter- and intramolecular hydrogen bond networks must be disrupted.

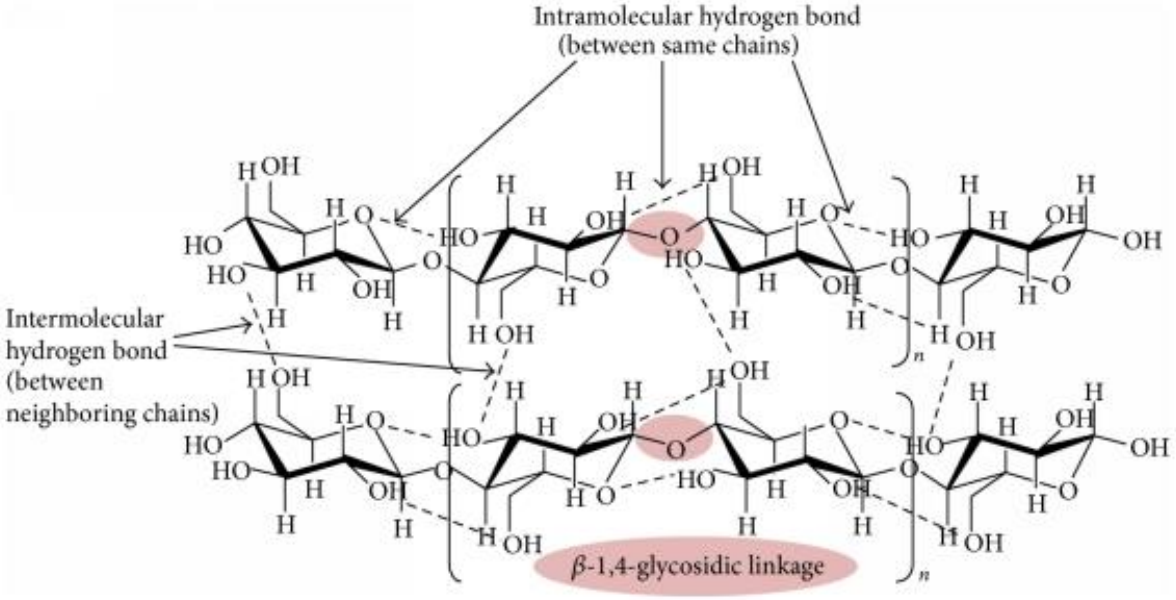

Figure 1: Molecular Structure of Cellulose and Its Hydrogen Bond Network

Ionic Liquids and EMImAC

Cellulose is notoriously difficult to solvate, as the extensive network of inter and intramolecular hydrogen bonds render it insoluble in water and common organic solvents [8]. Current industrialized solvent systems entail a variety of challenges, as some dissolution processes utilize volatile and hazardous organic compounds [9]. Other drawbacks of common solvents include excessive cost, high energy demands, difficulty in recovery and recycling, and environmental pollution [10]. A potential solution to these problems was found in a new class of cellulose solvents: room temperature ionic liquids (ILs). Ionic liquids are molten salts containing an organic cation and an inorganic anion. The cations in room temperature ionic liquids are polyatomic and asymmetric, and the ions are charge-diffuse and dispersed, which allows them to have a melting point below 100°C [11]. Unlike traditional solvents, ionic liquids are largely

nonvolatile, non-toxic, and can potentially be recycled through recovering the antisolvent by distillation [10]. A variety of ionic liquids have been found to dissolve cellulose, with the most effective solvents containing ammonium, phosphonium, pyridinium, and imidazolium cations, though ILs containing pyridinium ions can degrade cellulose if no protective gas is used [7]. Figure 2 depicts the chemical structure of the most common salts of each cation and their abbreviations, and figure 3 depicts the cation-anion pair of 1-ethyl-3-methylimidazolium (EMImAC, EMImOAc), the ionic liquid studied. The most common counterions studied include chloride, phosphate, acetate, and formate [11]. It has been suggested that the most effective ILs for cellulose dissolution belong to the 1-alkyl-3-methylimidazolium based solvents, especially 1-ethyl-3-methylimidazolium, which does not have a reactive side group and is less viscous than other aforementioned ILs [7]. Ionic liquids have not yet been adopted into commercial processes due to their high viscosities. The most commonly studied ILs have viscosities two to three orders of magnitude greater than those of conventional organic solvents, which complicates heat and mass transfer rates during processing and reduces the dispersion of cellulose throughout the system [8].

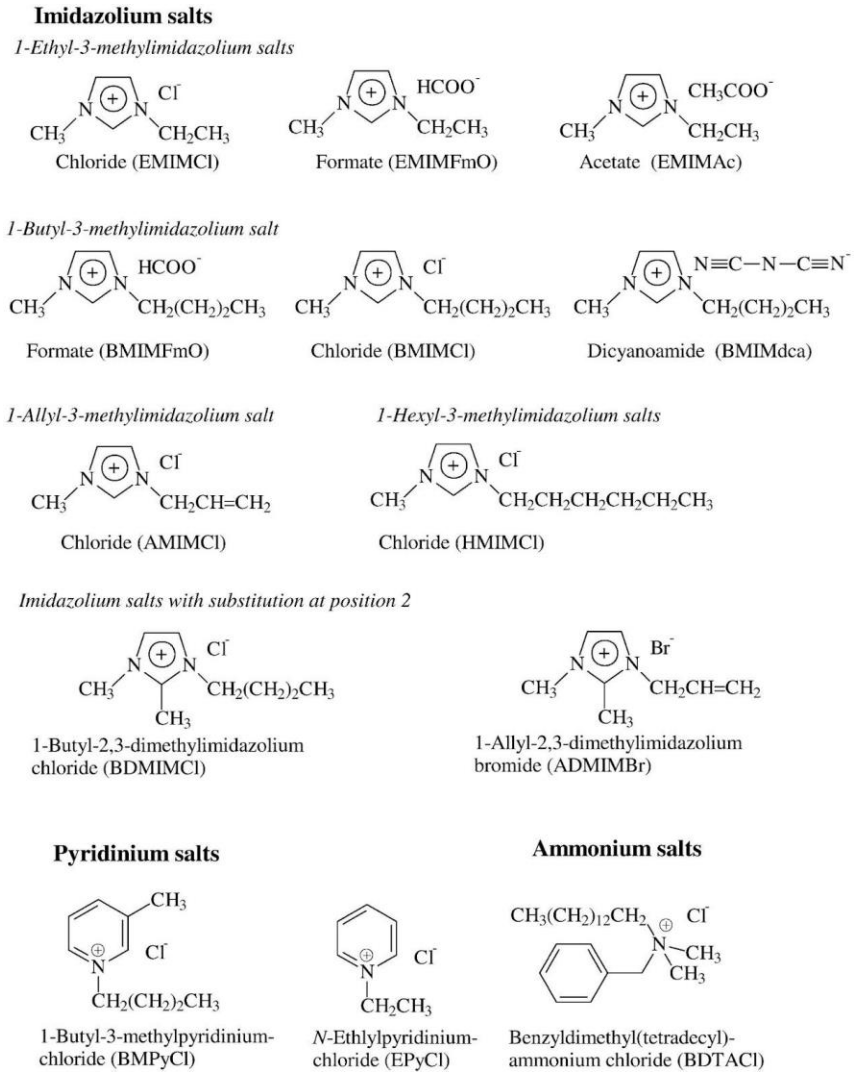

Figure 2: Chemical Structures of Common Ionic Liquids

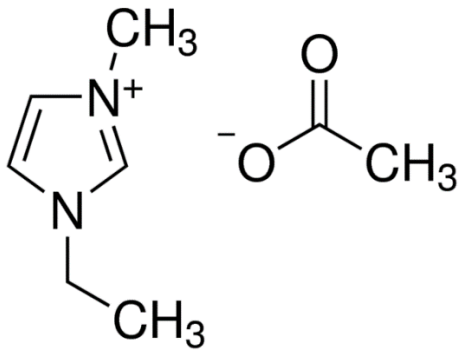

Figure 3: Molecular Structure of EMImAC

Dimethyl Sulfoxide

In order to reduce the viscosity of cellulose/IL solutions, a less viscous cosolvent can be incorporated. In order to avoid reducing the ionic liquid's efficacy in dissolving cellulose, the cosolvent must be aprotic and highly polar [12]. The most commonly utilized cosolvents in cellulose dissolution are pyridine, dimethylformamide (DMF), and dimethyl sulfoxide (DMSO). The addition of these cosolvents to ionic liquid systems has been studied for a wide range of solvents, and has been shown to significantly lower the viscosity of the system and increase the rate of dissolution for cellulose [11]. The chemical structure of DMSO, the cosolvent investigated in this study, is shown in figure 4.

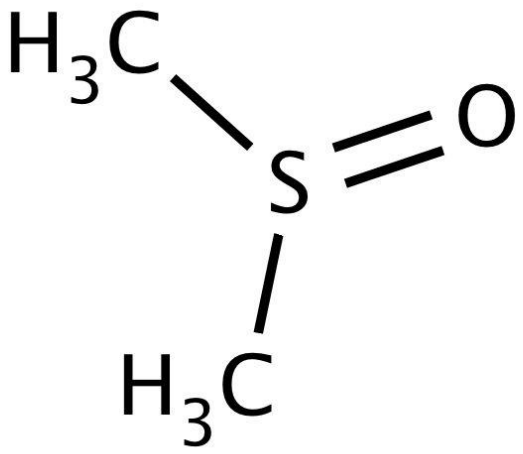

Figure 4: Molecular Structure of Dimethyl Sulfoxide (DMSO)

Chapter 2

Theoretical Background

This chapter explains the necessary theoretical background on polymer chemistry and physics to contextualize the experiments performed in this paper. Solvency conditions and chain dynamics in solution, viscosity and viscoelastic behaviors of polymers, and the rheological analysis of polymers will be discussed in the context of cellulose/IL solutions. The theoretical background will be utilized in the results and discussion section.

Polymer Solutions and Solvency

As the vast majority of applications for cellulose require its dissolution into a solvent, explaining the behaviors of polymers in solution is vital for a complete understanding of cellulose solutions. This section will outline key concepts governing the solubility of polymers and their behaviors in solution. The ideas discussed here will be used to evaluate the cellulose/ionic liquid/DMSO solutions in chapter 7.

Chain Conformations of Polymers in Solution

The conformation of a polymer in solution influences how the solution behaves during processing, and is thus critical to understand. The configuration of a polymer in solution is controlled by a variety of factors, namely the chemical structure of the monomer, the interactions between the polymer chains, the stiffness of the polymer chains, and the interactions between the polymer chains and the solvent [13]. The conformation of the polymeric chains changes

depending on the compatibility of the polymer and the solvent, as the solubility of a polymer in a particular solvent is determined by the interactions between the solvent and the polymer chain. Generally, the solubility increases with greater chemical and structural similarity between the solvent and the solute [13]. The polymer-solvent interactions determine the volume of the polymer coil in solution. A "good" solvent is highly compatible with the polymer, and will cause the polymer coil to expand due to the thermodynamic favorability of solvent-polymer interactions. A "poor" solvent will cause the polymer chains to remain tightly coiled, as the polymer will favor interacting with itself over the solvent [13]. In a theta (θ) solvent, the expansion and collapse of polymer chains is roughly equivalent, as the polymer-polymer and polymer-solvent interactions are equally preferred. The ionic liquid solvent studied in this paper, 1-ethyl-3-methylimidazolium acetate (EMImAC), has been determined to be a theta solvent [14].

Concentration Regimes

The concentration of a polymer in solution refers to the amount of polymer dissolved in the solvent compared to the amount of solvent. A polymer solution is classified as either dilute, semi-dilute, or concentrated based on the mass concentration *c* of the polymer in solution [15]. The concentration can also be quantified by the volume fraction of a polymer Φ , which is defined as the ratio of the amount of volume taken up by the polymer in solution to the volume of the solution [15]. The volume fraction can be written as:

$$\phi = \frac{c}{\rho} = c\left(\frac{v_{mon}\, N_{Av}}{M_{mon}}\right) \qquad \text{(Eq.1)}$$

where ρ is the density of the polymer, $v_{mon}N_{Av}$ is the monomer molar volume, and M_{mon} is the monomer molar mass [15]. The pervaded volume of a polymer V is the volume of solution spanned by the polymer chain, and is defined as:

$$V \approx R^3 \quad \text{(Eq. 2)}$$

where R is the size of the polymer chain. The pervaded volume is typically much larger than the occupied volume of the chain, as most of the pervaded volume is filled with solvent or other polymer chains. The overlap volume fraction Φ^* and the overlap concentration c^* are defined as the volume fraction or mass fraction of a single molecule within its pervaded volume [15].

$$\phi^* = \frac{Nv_{mon}}{V} \quad \text{(Eq. 3)}$$

$$c^* = \frac{\rho N v_{mon}}{V} = \frac{M}{V N_{Av}} \quad \text{(Eq. 4)}$$

When the polymer concentration c is below the overlap concentration c^*, the solution is classified as dilute. In dilute solutions, the average distance between polymer chains is larger than the size of the polymer chains and no chain entanglement occurs. Semi-dilute solutions contain polymer concentrations above that of the overlap concentration. Though most of the volume of semi-dilute solutions is occupied by the solvent, the polymer chains begin to overlap and greatly influence the properties of the solution, such as viscosity [15]. When individual chains begin to heavily overlap and become entangled, the solution is classified as entangled or concentrated. A depiction of the concentration regimes of a polymer in a good solvent (orange) and a poor solvent (blue) is depicted below in figure 5.

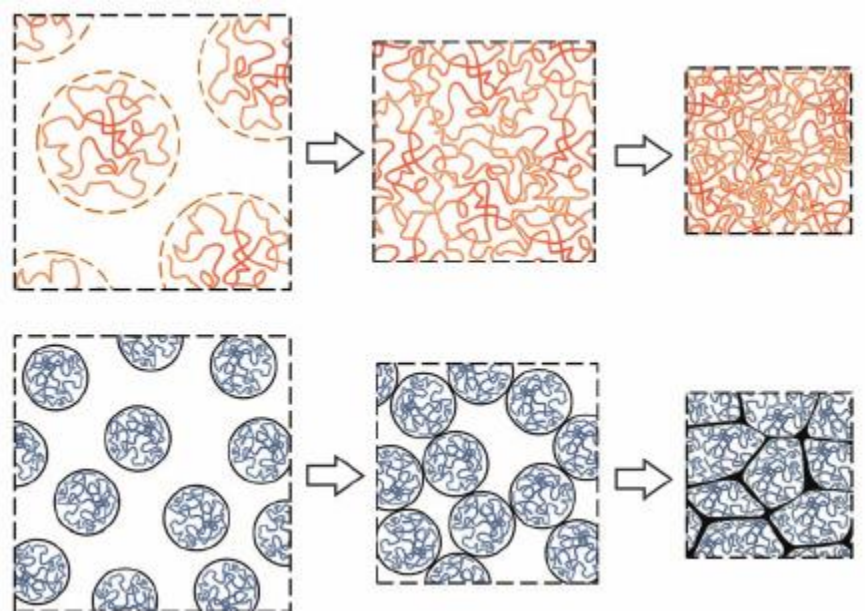

Figure 5: Concentration Regimes of a Polymer in a Good Solvent (top) and Poor Solvent (bottom). From left to right: dilute (c<c*), semi-dilute unentangled (c>c*), and semi-dilute entangled (c>>c*).

Kamlet-Taft Parameters

The dissolution of cellulose is highly influenced by the strength and structure of its network of hydrogen bonds, and ionic liquids function as cellulose solvents due to their ability to act as hydrogen bond donors/acceptors. Thus, understanding the ability of a solvent to interact with hydrogen bonds is critical in the study of cellulose/cosolvent/ionic liquid systems. The Kamlet-Taft parameters of a particular solvent quantify the solvent's ability to donate hydrogen bonds (acidity, α), accept hydrogen bonds (basicity, β), and undergo polarization/form dipoles (π^*) [16]. The acidity of an ionic liquid is correlated with the nature of the cation, while the basicity is correlated with that of the anion. Generally, the values of the parameters range from 0 to 1, with larger values indicating a greater ability to donate hydrogen bonds, accept hydrogen bonds, and undergo polarization, respectively. Table 1 below lists the Kamlet-Taft parameters of

EMImAC, which is the ionic liquid used in this study. EMImAC is one of few ionic liquids that can dissolve cellulose due to its anomalously high β value, as the acetate ion is an extremely strong hydrogen bond acceptor [12].

Table 1: Kamlet-Taft Parameters of EMImAC

Solvent	α	β	π^*
EMImAC	0.4	0.95	1.09

Polymer Chain Dynamics and Associations

The next section discusses the behaviors of polymer solutions exposed to stress and strain, which dictate the processing ability of the solutions.

Viscoelasticity

Polymers, in contrast to other types of materials, do not have a linear, time-independent response to applied stress σ or strain γ [17]. Polymers are characterized by their viscoelastic behavior, meaning that they behave like elastic solids at low temperatures and high frequencies and viscous liquids at high temperatures and low frequencies. Elastic solids follow Hooke's law, which states that applied stress is directly proportional to strain. The factor of proportionality in Hooke's law, G, is the elastic modulus of the material. Viscous liquids do not follow Hooke's law but instead obey Newton's law for viscous liquids, which states that the stress is proportional to the strain rate $\dot{\gamma}$. The factor of proportionality in Newton's law for viscous liquids is viscosity η.

$$\sigma = G\gamma \quad \text{(Eq. 5)}$$

$$\sigma = \eta\dot{\gamma} \quad \text{(Eq. 6)}$$

Linear viscoelasticity in a polymer is exhibited when the stress is linearly proportional to the strain, and thus the modulus G is independent of strain. Experiments conducted in a polymer's linear viscoelastic regime are essential for determining the characteristics of the polymer and can be used to inform how the polymer is processed. Of the three main linear viscoelastic experiments, oscillatory shear is the one most relevant to this study. Oscillatory shear tests can be performed on a rheometer by applying a sinusoidal strain γ at an angular frequency ω to a sample.

$$\gamma = y_0 \sin(\omega t) \quad \text{(Eq. 7)}$$

The stress on the sample will then gradually approach a steady sinusoidal stress σ.

$$\sigma = \gamma_0[G'(\omega)\sin(\omega t) + G''(\omega)\cos(\omega t)] \quad \text{(Eq. 8)}$$

The rheometer measures the magnitude of the complex modulus $|G^*| = G_d$ and the phase angle δ, which are then used to calculate the loss tangent tan(δ), the storage modulus G', the loss modulus G", and the complex viscosity $\eta^*(\omega)$ through the following equations:

$$G^*(\omega) = G"(\omega) + iG'(\omega) \quad \text{(Eq. 9)}$$

$$G_d = |G^*| = \sqrt{(G')^2 + (G")^2} \quad \text{(Eq. 10)}$$

$$tan(\delta) = \frac{G"}{G'} \quad \text{(Eq. 11)}$$

$$G' = G_d cos(\delta) \qquad G_d = \frac{\sigma_0}{\gamma_0} \quad \text{(Eq. 12)}$$

$$G" = G_d sin(\delta) \qquad G_d = \frac{\sigma_0}{\gamma_0} \quad \text{(Eq. 13)}$$

$$\eta^*(\omega) = \frac{G^*(\omega)}{i\omega} \quad \text{(Eq. 14)}$$

A typical rheometer will plot the storage modulus, loss modulus, and phase angle as a function of the log of frequency. The storage modulus G' indicates the sample's elastic response, while the loss modulus G" indicates the viscous behavior. Thus, when the storage modulus G' is higher than the loss modulus G", the polymer's behavior is classified as elastic and solid-like. A storage modulus less than the loss modulus indicates that the polymer's behavior is liquid-like. A viscoelastic liquid like a polymer solution will exhibit liquid-like and solid-like responses. Figure 6 depicts the results of an oscillatory shear test (frequency sweep) performed on a viscoelastic solid, a gel, and a viscoelastic liquid [18].

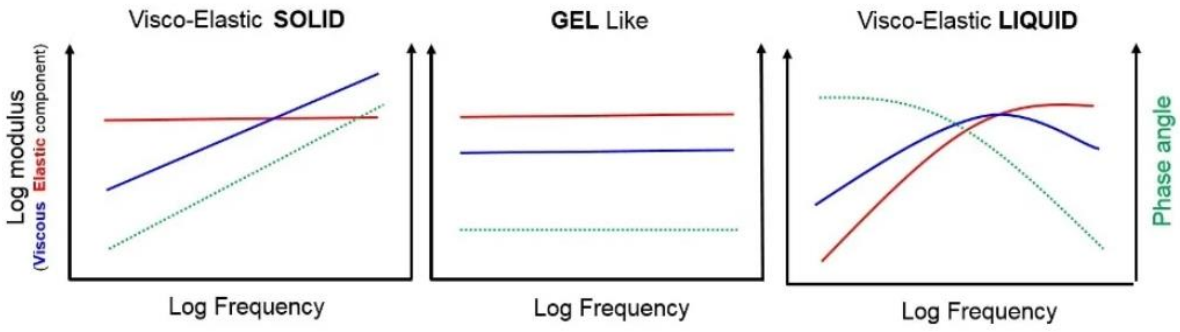

Figure 6: Oscillatory Shear Test Results Performed on a Viscoelastic Solid (left), a Gel (center), and a viscoelastic liquid (right)

Viscosity

The viscosity η of a material is defined as its resistance to applied stress. A polymer's viscosity is one of its most important properties, as the viscosity governs the suitable processing methods and applications of the polymer.

The origin of viscoelasticity is the molecular motion of polymeric chains. The relatively large size of polymer molecules and the high number of intermolecular interactions between chains allows the material to resist deformation and flow despite the flexibility of the chains themselves [19]. The viscosity of a polymer solution is influenced by the polymer's molecular weight, concentration, chain length, entanglements, crosslinks, branches, and the inter- and intramolecular interactions present. As noted in the previous section, polymer solutions in the dilute regime have more free volume, which decreases the viscosity.

Table 2 depicts several forms of viscosity used to characterize polymer solutions in dilute regimes. The most important viscosity in the study of dilute solutions is the intrinsic viscosity [η], which quantifies the ability of a polymer to increase the viscosity of a solvent at a particular temperature [20]. However, the intrinsic viscosity is not a true measure of the solution's

viscosity. The intrinsic viscosity is actually taken from the initial slope of either the relative viscosity or the specific viscosity as a function of concentration at a given temperature.

Table 2: Forms of Viscosity and Their Definitions

Name	Definition
Relative Viscosity	$\eta_r = \frac{\eta}{\eta_0}$
Specific Viscosity	$\eta_{sp} = \eta_r - 1$
Reduced Viscosity	$\eta_{red} = \frac{\eta_{sp}}{c}$
Inherent Viscosity	$\eta_{inh} = [\frac{ln(\eta_r)}{c}]$
Intrinsic Viscosity	$[\eta] = \lim_{c \to 0} \eta_{red} = \lim_{c \to 0} \eta_{inh}$

The specific viscosity η_{sp} of a polymer solution of concentration c is given as:

$$\eta_{sp} = k_0[\eta]c + k_1[\eta]^2c^2 + k_2[\eta]^3c^3 + \ldots \quad \text{(Eq. 15)}$$

where $[\eta]$ is the intrinsic viscosity, and k_0 through k_n are dimensionless constants (k_0=1) [10]. This equation can be reduced into the Huggins equation, which is valid for dilute solutions ($[\eta]c << 1$).

$$\frac{\eta_{sp}}{c} = [\eta] + k_H[\eta]^2c \quad \text{(Eq. 16)}$$

k_H is the Huggins constant, which represents the favorability of a particular solvent-polymer system and is relatively independent of molar mass [20]. The Huggins constant ranges from 0.3 for good solvent-polymer systems to 0.5 for poor solvent-polymer systems.

Using the definitions in Table 2, the Huggins equation can also be arranged into the Kraemer equation, which defines the inherent viscosity:

$$\eta_{inh} = \frac{ln(\eta_r)}{c} = [\eta] + k_K[\eta]^2 c \qquad \text{(Eq. 17)}$$

In this equation, k_K is called the Kraemer parameter and is calculated through the equation $k_K = k_H - ½$. k_K is either a negative value or 0.

The Huggins and Kraemer equations can be used to evaluate experimental data to determine the [η] of a polymer solution. Both equations are plotted against the concentration of a sample and extrapolated to the y-intercept of the graph, which gives the intrinsic viscosity of a solution [20]. The intrinsic viscosity can then be used to calculate the viscosity average molar mass M_V from the Mark-Houwink-Sakurada equation.

Shear-Thinning Behavior

The discussion in the previous section centered on linear viscoelastic behavior of polymer solutions. Though this model holds well at small deformations and low shear rates, the majority of polymers exhibit shear-thinning behavior [19]. As opposed to simple Newtonian fluids, in which viscosity is independent of strain rate, shear-thinning liquids exhibit a decrease in viscosity with increasing shear rate [19]. The origin of shear-thinning behavior lies in the

polymer's intermolecular interactions: as a shear force is applied, the material relieves stress by breaking some intermolecular interactions and disentangling polymer chains. Continual force prevents the intermolecular interactions from reforming, and with fewer associations, the material weakens further.

The dependency of viscosity on shear rate can be described through several mathematical models. The power law model is the most basic model and was derived empirically. In the power law model, the viscosity η is related to shear rate $\dot{y}$ though Equation 18, in which k_f is the consistency factor and n is the flow behavior index (n=1 for Newtonian fluids, 0<n<1 for shear-thinning liquids, and n>1 for shear-thickening fluids). The power law model is limited in that it does not accurately represent the Newtonian portion of a solution's flow profile, and has thus been modified. The Cross (Eq. 19) and Carreau models (Eq. 20) were both developed to include a wider range of shear rates that more accurately reflect Newtonian behavior [21]. In both models, η_0 is the zero-shear viscosity and τ is the terminal relaxation time of the polymer system. More models exist to describe specific cases, such as behavior near the high shear limiting viscosity or polymer systems with a broad molecular weight distribution, but these are not relevant to this experiment and will not be discussed further.

Power Law (Ostwald-de Waele) Model: $$\eta(\dot{y}) = k_f \, \dot{y}^{n-1} \qquad \text{(Eq. 18)}$$

Cross Model: $$\eta(\dot{y}) = \eta_0[1 + |\tau\dot{y}|^m]^{-1} \qquad \text{(Eq. 19)}$$

Carreau Model: $$\eta(\dot{y}) = \eta_0[1 + |\tau\dot{y}|^2]^{(n-1)/2} \qquad \text{(Eq. 20)}$$

Chain Associations

Just as there are several models for describing the viscosity of a solution, several models have been proposed to model polymer chain dynamics. These models depict the relaxation times and viscosities of polymer solutions. Though several models exist and describe a wide spectrum of behaviors, this paper will focus on two models for unentangled polymer solutions, as the samples evaluated in this study are well below the overlap concentration and in the dilute regime.

The Rouse Model

The Rouse model was one of the first theories on the movement and dynamics of polymer chains [22]. The model assumes that the polymer can be accurately described by a series of *N* beads connected to each other by *N-1* springs of size *b*, which are governed by Hooke's law. The motion of the polymer chains is controlled by three forces acting on the repeat units: a frictional force proportional to the relative viscosity of the solution, the force between repeat units along the chain, and a random force arising from collisions between the solvent and polymer chains due to Brownian motion [22]. The diffusion coefficient of the polymer chain is related to the resistance of the monomers, which governs the viscosity, and the temperature T. Each bead has a friction coefficient of ζ, and the total friction coefficient of the chain is equivalent to the sum of each bead's coefficient. The friction and diffusion coefficients are related to the Rouse relaxation time τ_R, which is the time needed for the polymer chain to diffuse a distance of its own size R. The equations defining the Rouse model are given below.

Total Friction of the Polymer Chain: $$\zeta_R = N\zeta \quad \text{(Eq. 21)}$$

Rouse Diffusion Coefficient: $$D_R = \frac{kT}{\zeta_R} = \frac{kT}{N\zeta} \quad \text{(Eq. 22)}$$

Rouse Relaxation Time: $$\tau_R \approx \frac{R^2}{D_R} \approx \frac{kT}{N\zeta};\ R = bN^{1/2} \quad \text{(Eq. 23)}$$

The Rouse model can be used to determine the solvent viscosity η_s by incorporating the Kuhn monomer relaxation time τ_0 and Stokes law for the friction coefficient of the monomer:

Kuhn Monomer Relaxation Time: $$\tau_0 \approx \frac{\zeta b^2}{kT} \quad \text{(Eq. 24.1)}$$

$$\tau_R \approx \frac{\zeta}{kT} NR^2 \approx \frac{\zeta b^2}{kT} N^2 \quad \text{(Eq. 24.2)}$$

Stokes Law: $$\zeta \approx \eta_s b \quad \text{(Eq. 25)}$$

Rouse Model: $$\tau_R \approx \frac{\eta_s b^3}{kT} N^2 \quad \text{(Eq. 26)}$$

In a dilute system, the motion of a polymer molecule affects both the rest of the polymer chain and the solvent surrounding it. When a particle moves, it moves some of the surrounding media with it, causing the solvent to viscously resist the motion [23]. The particle will also interact with the other beads on the polymer chain. The Rouse model ignores the hydrodynamic interaction between particles and the solvent, and assumes that the polymer beads only interact through the spring connecting them [23]. This limits the application of the Rouse model in dilute

systems where solvent-particle interactions are of high importance. The Rouse model is used to model semidilute unentangled solutions with concentrations between c* and c^e, where the entanglement concentration c^e is approximately 10c*.

The Zimm Model

The Zimm model attempts to more accurately model the behavior of a polymer in a dilute solution by accounting for hydrodynamic interactions between the monomers and the solvent. In the Zimm model, the pervaded volume of the polymer chain, which was discussed previously, is treated like a solid object of size $R \approx bN^{\nu}$ moving through the solvent, where the parameter v is the pervaded volume of the chain. Like the Rouse model, the diffusion and friction coefficients are used to calculate the relaxation time. The Zimm relaxation time is similarly defined as the amount of time required for a polymer chain to diffuse a distance equal to its size. The equations defining the Zimm model are listed below:

Friction Coefficient of the Chain: $$\zeta_z \approx \eta_s R \quad \text{(Eq. 27)}$$

Diffusion Coefficient of the Chain: $$D_z = \frac{kT}{\zeta_z} \approx \frac{kT}{\eta_s R} \approx \frac{kT}{\eta_s b N^{\nu}} \quad \text{(Eq. 28)}$$

Zimm Relaxation Time: $$\tau_z \approx \frac{R^2}{D_z} \approx \frac{\eta_s}{kT} R^3 \approx \frac{\eta_s b^3}{kT} N^{3\nu} \approx \tau_0 N^{3\nu} \quad \text{(Eq. 29)}$$

As the Zimm model reflects the behavior of a polymer in a dilute solution, the model and thus the Zimm relaxation time τ_z is dictated by how well the polymer and solvent interact, as the interaction between the polymer and solvent dictate the pervaded volume. The Zimm relaxation time can therefore be described for chains of different lengths. Short chains, which are defined as having a length of $N < b^6/v^2$, have an exuded volume closer to that of a θ solvent. The Zimm model is used to model dilute solutions in which the concentration is less than c*.

$$\tau_z = \frac{\eta_s R^3}{kT} \approx \begin{cases} \tau_0 N^{3/2}\,; & N < b^6/v^2 \\ \tau_0 (v/b^3)^{6v-3} N^{3v}; & N < b^6/v^2 \end{cases} \qquad \text{(Eq. 30)}$$

Chapter 3

Literature Review

This section discusses the current research on cellulose and ionic liquid systems, the proposed mechanisms of cellulose dissolution, and the effect of cosolvents on the properties and behavior of cellulose/IL solutions. Additionally, the fiber-spinning process and fabrication of fibers from cellulose/ionic liquid solutions is discussed. The overview of current research will be used to contextualize the results reported in chapter 7 and will be utilized to explain the behavior of the samples studied in this experiment.

Cellulose Dissolution in Ionic Liquids

It is widely accepted that in order to dissolve cellulose, the network of inter- and intramolecular hydrogen bonds must be disrupted. Traditional dissolution methods break the hydrogen bonding network through functionalization reactions (e.g. nitration, esterification) with the hydroxyl groups on the cellulose chain [24]. Ionic liquid solvents, however, do not chemically modify the cellulose molecules. ^{13}C NMR experiments have shown that no covalent bonds are formed between the solvent and cellulose chains, so ionic liquids are widely considered non-derivatizing solvents [1]. Beyond the consensus that ionic liquids are non-derivatizing solvents, there is little agreement on how ionic liquids dissolve cellulose and what interactions occur between the ionic liquid and the cellulose molecule [1].

It was first argued that the cation contributed little to the dissolution of cellulose in ionic liquids, and that the anion was the main factor in controlling the solubility and dissolution rate [25]. Several studies have suggested that the anion in ionic liquids plays a more significant role

in cellulose solvation through disrupting the inter- and intramolecular hydrogen bonding system [26]. For example, research on acetate-based ionic liquids proposed that the ionic liquid dissolves cellulose by forming hydrogen bonds between the anions and primary hydroxyls of cellulose [27]. This model of anion-cellulose hydrogen bonding has been widely accepted for most ionic liquids. After the anions hydrogen bond with the cellulose hydroxyls, the anion-cellulose complexes, now negatively charged, repel from each other and are surrounded by the large cations to maintain electroneutrality [28]. This dissolution process is depicted in figure 7, which shows the dissolution of cellulose (green) by the ionic liquid 1-(n-butyl)-3-methylimidazolium acetate (red and blue) and the cosolvent dimethyl sulfoxide (black) [28]. The most effective solvents contain anions that are relatively small and good hydrogen bond acceptors [25]. Strongly electronegative anions such as Cl^- were found to have better dissolution abilities than non-coordinating anions like $[BF_4]$ [11].

The role of the cation in cellulose dissolution is more disputed, though it appears to play an integral part in the dissolution process [12]. In a study of four imidazolium-based ionic liquids, it was determined that cellulose solubility decreased with increasing alkyl chain length in the imidazolium cation [27]. Increased alkyl length in the cation increases the acidity of the hydrogen atoms in the imidazolium cation, which effects the dissolution of cellulose by controlling the formation of hydrogen bonds between the cation's acidic hydrogen and cellulose's hydroxyl oxygen [27]. Additionally, the presence of electronegative atoms on the cation decreases the solvation efficiency by decreasing the acidity of the protons [25]. The most effective solvents utilize cations with strong acidic protons with no electronegative atoms.

Based on this data, it has been concluded that the most effective IL solvents of cellulose are 1-alkyl-3-methylimidazolium- and 1-alkyl-3-methylpyridinium-based ionic liquids with short alkyl substituents ranging from C2 to C7 containing either acetate or chloride counterions [11]. Due to the higher melting point and viscosity of chloride-based ionic liquids, 1-ethyl-3-methylimidazolium acetate (EMImAC) was chosen as the solvent for this experiment.

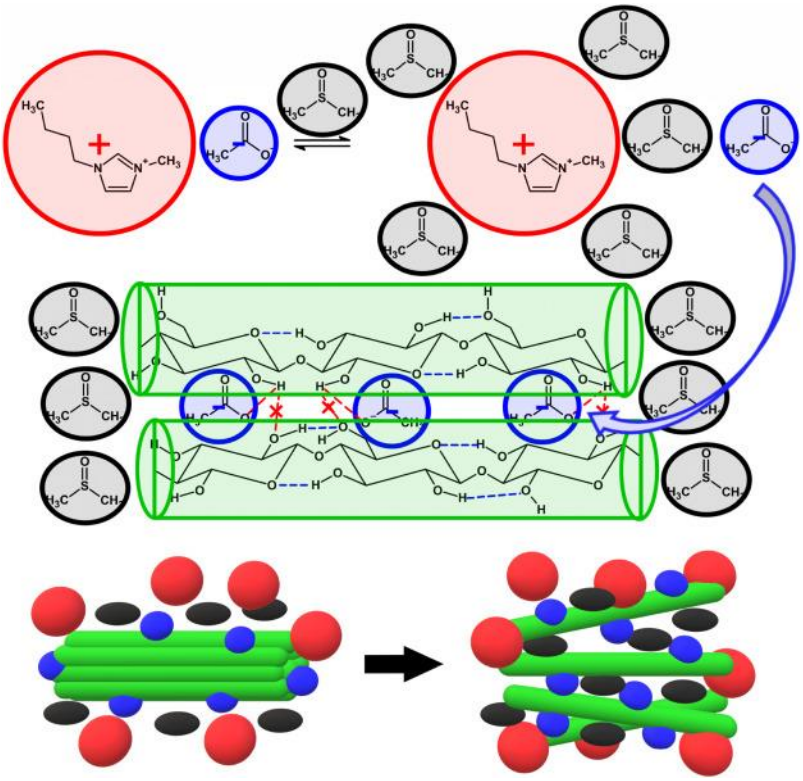

Figure 7: Dissolution of Cellulose (Green) in 1-(n-butyl)-3-methylimidazolium acetate (red, blue) and DMSO (black)

Cosolvent Effect on Cellulose/IL Solutions

As previously discussed, one of the main disadvantages of using ionic liquids as cellulose solvents is their high viscosities, which complicates further processing. In order to reduce the viscosity of cellulose/IL solutions, less viscous cosolvents can be added to the system. Recent

research has shown that the addition of polar, aprotic cosolvents like dimethylformamide (DMF) and dimethyl sulfoxide (DMSO) dramatically reduces the viscosity of the system without compromising the efficacy of cellulose dissolution [8]. Tomimatsu et al. determined that the addition of DMSO to various cellulose/IL systems increased the solubility of cellulose as well as the speed of dissolution [12].

The dissolution of cellulose in binary IL/cosolvent systems is still governed by the hydrogen bond interaction between the anions and hydroxyl protons of cellulose, as the cosolvent only indirectly affects cellulose's solubility by altering the interactions between the anion and cellulose molecules [2]. Aprotic cosolvents increase the concentration of the free anions due to preferential solvation of the cation by aprotic polar solvents [26]. The aprotic solvents were theorized to solvate the ion pairs in the IL, which increased cellulose solubility by removing the cation from the ion pair and thus increasing the interaction between the anion and cellulose [29]. In contrast, protic solvents decreased the solubility of cellulose by favorably interacting with the anions and thus reducing the interaction between the anions and cellulose [2]. The size of the cosolvent molecule also controls the solvation of cellulose in IL/cosolvent systems, as larger cosolvents like DMSO were more effective than cosolvent molecules of smaller molar volumes [2]. DMSO decreases the system's viscosity without altering the interactions between the cation/anion pairs or the interactions between the ionic liquid and cellulose by increasing mass transport [27]. As DMSO was found to be an ideal cosolvent for ionic liquid/cellulose systems, it was utilized in this experiment.

Other Factors Influencing Cellulose Dissolution

Factors other than the composition of the solvent and the inclusion of a cosolvent affect the solubility of cellulose in ionic liquid, though the solvent/cosolvent plays the most important role. Numerous studies have shown that increasing the temperature of the system reduces the dissolution time, though the ideal length of time and temperature is still subject to debate [11]. As previously reported by Utomo et al, the prolonged storage (>5 days) of cellulose/IL solutions at temperatures above 85°C can cause the degradation of cellulose [30]. The presence of water, a nonsolvent of cellulose, also reduces the dissolution of cellulose by interfering with the cellulose's ability to hydrogen bond to the anion in the ionic liquid [31]. In order to mitigate the effects of both temperature and water content on the solutions, the samples prepared in this experiment were heated to 80° for 5 days before testing to allow the full dissolution of cellulose and the elimination of moisture in the system.

Chapter 4

Fiber-Spinning

One of the main areas of interest for cellulose processing is in the production of fibers through the process of fiber-spinning. Ionic liquid/cellulose solutions, called dopes, can be spun into textile fibers through several types of spinning processes. Dry-spinning, wet-spinning, dry-jet-wet spinning, and electrospinning techniques have all been used to create cellulose fibers in micro- and nano- dimensions, though the insolubility of cellulose in common solvents has prevented the commercial production of pure cellulose fibers [32].

Fiber-Spinning Techniques

The main fiber-spinning techniques employed by industry today, wet-spinning, dry-spinning, and melt-spinning, are characterized by how they produce fiber from dope and the size of the fiber produced. Melt-spinning forms fibers by forcing the dope through a die, called the 'spinneret', at high pressures [33]. The dope in melt-spinning is usually the melted polymer and additives if necessary. The fibers are then stretched and drawn to the desired diameter and hardened by cooled air. As cellulose does not melt due to its hydrogen bonding network, melt-spinning cannot be used to spin cellulose into fibers and will not be discussed in this paper. Unlike melt-spinning, wet-spinning and dry-spinning both utilize dopes made from polymers dissolved in solvents. Solutions utilized in dry-spinning are made with volatile solvents that evaporate when the fiber is extruded into air [21]. In contrast, wet-spinning extrudes the fiber into a liquid bath of coagulating agents that drive off the solvent. Traditional methods of manufacturing cellulose fibers, namely the viscose process, utilize wet-spinning due to

cellulose's resistance to melting and dissolution [33]. The wet- and dry-spinning techniques can be combined into the dry-jet-wet spinning (also known as "air gap spinning") process. In dry-jet-wet spinning, an air gap is maintained between the end of the spinneret and the coagulation bath [33]. This process increases the strength and stiffness of the fiber product, as the polymer chains orient themselves in an anisotropic domain as the fiber passes through the air gap [33]. Both wet-spinning and dry-jet-wet spinning systems generally utilize water, alcohols, or less polar solvents like acetone as coagulators [34]. As the wet-spinning and dry-jet-wet spinning techniques have been successfully applied to cellulose/IL systems, this paper will focus namely on these processes.

One fiber-spinning technique that has recently garnered interest due to its ability due to its ability to produce nanofibers is electrospinning [35]. Electrospinning produces fibers by exerting a high-voltage external electric field on the surface of a polymer melt or solution [36]. The micro/nanofibers manufactured by electrospinning are characterized by high surface to volume ratios, which impart a range of highly desirable properties [35]. The potential utilization of biocompatible cellulose nanofibers in biomedical applications has revitalized the study of electrospinning [32], and this process will be discussed alongside wet- and dry-wet-jet spinning in this paper.

Factors Affecting Spinnability of Solutions

The polymer dope's ability to form fibers through a particular spinning technique is referred to as its spinnability. Among other factors attributed to the specific spinning process (the draw ratio, temperature of the coagulation bath, air gap length), the spinnability of a particular

solution depends on the characteristics of its flow, its crystallinity, and its rheological behaviors. The rheological behavior of a solution correlates with the entanglement and relaxation of the polymer solution, which in turn dictates the orientation of the crystalline and amorphous regions of the polymer [37]. As previously noted, the orientation and alignment of crystalline sections controls the strength and stiffness of the fiber, and are thus critical parameters. Additionally, the solution should exhibit shear-thinning behavior upon applied shear stress such that high-throughput extrusion of the dope can occur in the spinneret without the production of high pressures [38].

The dopes utilized in any spinning process, but especially in dry-jet-wet spinning, must have a balance of elastic behavior and viscous fluidity [38]. The solution must be viscoelastic enough to withstand filament drawing in dry-jet-wet spinning- if the filament is too thin, the fiber will collapse or break when ejected from the spinneret, and no fiber will be formed [38]. The wet-spinning process requires relatively low viscosities (zero-shear viscosities of approx. 5-20 Pas) because the fiber is ejected directly into the coagulator bath [3]. However, air gap spinning requires dopes of much higher viscosities (approx. 5,000-30,000 Pas at spinning temp) so that the filament can withstand the uniaxial stress exerted during the drawing process in the air gap [39].

Fiber-Spinning of Cellulose/Ionic Liquid Solutions

Although fibers have been spun from 1-butyl, ethyl or allyl-3-methylimidazolium ionic liquids, like [BMIm]Cl, [EMIm]Cl, [EMIm]AC and [AMIm]Cl,11,17–21 and from [DBNH]AC

(1,5-diazybicyclo[4.3.0]nonenium acetate), the wide scale implementation of IL solvents for cellulose is still not possible [3]. Fiber-spinning of cellulose is hindered by the same lack of nonvolatile, nontoxic solvents that prevents cellulose dissolution and processing in other areas. Although the use of ionic liquids as solvents is promising due to the nontoxic, biodegradable, and recyclable nature of ionic liquids, the highly viscous cellulose/IL dopes cannot be spun efficiently. The spinning process for cellulose/IL solutions is difficult to control for continuous jets, as the high viscosities and ionic strength of the solutions can cause complications such as adhesion and contraction of the wet fibers, during the spinning process [35]. Another major complication resulting from the high viscosities of IL/cellulose dopes is the need for high dissolution and processing temperatures. Reducing the viscosity of these solutions by increasing the processing and dissolution temperatures can cause the decomposition of the ionic liquids and the degradation of the cellulose polymers even if stabilizers are added [38].

Cosolvent Effect

The addition of cosolvents, especially DMSO, has similarly improved the outlook on cellulose spinning by reducing the dope viscosity, surface tension, and entanglement density of the network [35]. A study by Xu et al. examining the effect of the addition of DMSO as a cosolvent in cellulose/1-allyl-3-methylimidazolium chloride determined that the cosolvent also increased the conductivity of the dope, which facilitated the electrospinning process [35]. Lee et al. produced cellulose fibers from EMImAC solutions via the wet-spinning process, and demonstrated that the presence of DMSO or DMF in EMImAC solutions increased the dissolution rate of cellulose, reduced the complex viscosity, and increased the crystallinity of the

fibers as a result of interaction between cellulose chains. The cosolvents also increased the mobility of the cellulose chains and the tensile strain due to the plasticization effect [6].

Chapter 5

Materials and Sample Preparation

Cellulose

The native cellulose sample studied in this investigation, $cell_{625}$, was obtained from Dow, Inc. (Midland, MI). The cellulose in $cell_{625}$ originated from cotton linters. The molecular weight of the sample is listed as 625 kg/mol. The intrinsic viscosity [η] of $cell_{625}$ in Cuen is 17.9 dL/g as evaluated by Dow, Inc. The cellulose samples were processed by Dow such that the majority of the hemicellulose and lignin were removed.

EMImAC

The 1-ethyl-3-methylimidazolium acetate (EMImAC) used in this study was purchased from IOLITEC (Heilbron, Germany). The contents provided by the manufacturer is >95% with <1% as analyzed via Karl Fischer titration [40]. The zero-shear viscosity and the glass transition temperatures obtained from the peak of the loss modulus G_{max}" and loss tangent $\tan(\delta)_{max}$ as determined by Uomo are listed in the table below [30]. According to the technical data sheet provided by IOLITEC, EMImAC has a density of 1.10g/mL at 25°C [40].

Table 3: Zero-Shear Viscosity and Glass Transition Temperatures of EMImAC

Ionic Liquid	Zero-Shear Viscosity at 30°C (Pa·s)	T_g (peak of the loss modulus G_{max}") (°C)	T_g (peak of loss tangent $\tan(\delta)_{max}$) (°C)
EMImAC	0.089	-68	-44

DMSO

The anhydrous dimethyl sulfoxide (DMSO) used in this experiment was obtained from Sigma-Aldrich (Saint Louis, MO). The sample is reported to be ≥ 99.9% pure with less than 0.005% water content, and has a density of 1.10 g/mL according to the product specification sheet provided by Sigma-Aldrich [41].

Methods of Sample Preparation

The cellulose and EMImAC were stored in a 40°C oven under vacuum overnight before sample preparation in order to eliminate residual moisture. DMSO was stored in a temperature-controlled glovebox under vacuum. All samples were 12mL, with varying concentrations of cellulose and DMSO in EMImAC, due to the sample volume requirements of the intrinsic viscometer. Both samples with and samples without DMSO were prepared by adding the EMImAC and/or DMSO to the cellulose in one of two methods described below. All of the samples without DMSO were stirred at room temperature for 5 minutes and then placed in the 80°C oven for 5-7 days to anneal. The samples containing DMSO were not placed in the 80°C oven. Samples with DMSO were prepared by first adding the DMSO to the cellulose, stirring the sample with a magnetic stir bar for 3 minutes, then adding the EMImAC, and then stirring the full sample for 5 minutes. Samples without DMSO were stirred after the EMImAC was added to each vial.

Aging and Degradation Concerns

Previous studies performed by the Colby laboratory have found that extended storage of cellulose/IL samples were prone to degradation when kept at 80°C [30] [42]. EMImAC/cellulose solutions were particularly prone to degradation in comparison to solutions made from other ionic liquids due to acid hydrolysis, which causes depolymerization. Utomo et al. reported that the cellulose in EMImAC solutions experienced a molecular weight decrease of 59% after being stored at 80°C, in comparison to only a 18% decrease when stored at 40°C [30]. Due to this observed degradation, the paper recommended that the maximum amount of time for EMImAC/cellulose samples be kept at 80°C be limited to 6 days. However, these samples had much higher concentrations of cellulose (1wt% cellulose samples as compared to the 0.3-0.05wt% cellulose samples studied in this experiment), which could mean that these degradation rates are not accurate for this study. That being said, no sample was stored at 80°C for longer than 6 days as a precautionary measure.

Homogeneity of Samples

Previous studies in the Colby lab prepared cellulose/IL samples with no stirring and an annealing period of 24 hours. Due to the inability to replicate tests, the samples from these studies were suspected to contain a concentration gradient of cellulose as well as residual moisture. In order to eliminate non-uniform dissolution of cellulose, all samples were stirred for at least 5 minutes with a magnetic stir bar.

The development of a concentration gradient within the samples was of particular concern in this study due to the large volume of sample compared to the low weight percent of

cellulose. Samples in previous papers that did not utilize the capillary rheometer were typically 3g (roughly 3.5mL) in size in order to reduce waste, limit the effects of water, and inhibit the development of a concentration gradient. However, the mini automated capillary rheometer utilized in this experiment uses a much higher volume of sample (12mL). In order to develop a new standard method of sample preparation, two potential avenues were explored and compared for the 0.3wt% cellulose/EMImAC sample. The first method, henceforth referred to as the "1 vial method", added all 12mL of EMImAC directly to the cellulose. The sample was then stirred at medium speed and visually inspected to ensure that no large cellulose particles remained. The second method, termed the "3 vial method", split the cellulose and EMImAC equally among 3 vials that were stirred and annealed in the oven separately. The contents of the vials were joined before loading the sample into the capillary viscometer. Figure 8 below depicts the results of testing each sample in the capillary rheometer to determine the intrinsic viscosity. As the 3 vial method had a higher viscosity than the 1 vial method, suggesting that the cellulose was more completely dissolved throughout the sample. Therefore, the 3 vial method was used to prepare all of the cellulose samples that did not contain DMSO.

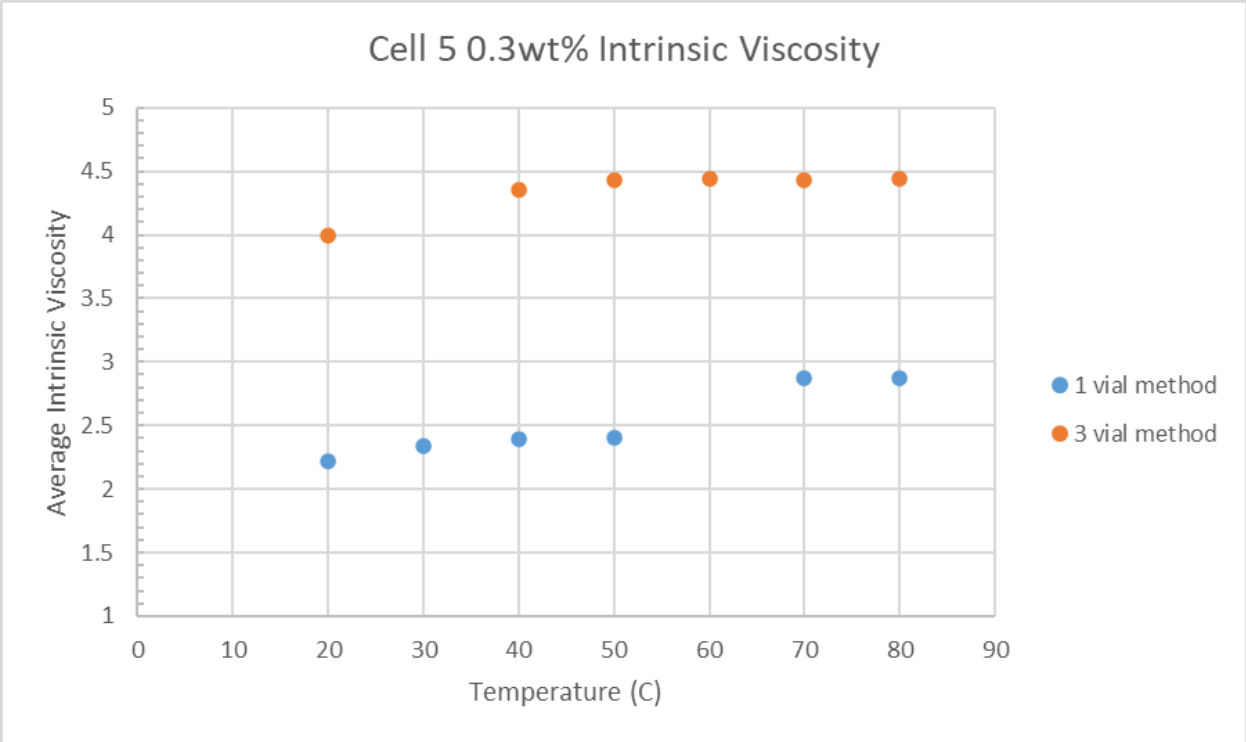

Figure 8: Comparison of the intrinsic viscosities for samples prepared via the 3 vial method (orange) and the 1 vial method (blue) for 0.3wt% cellulose samples without DMSO

The samples containing DMSO were similarly studied by comparing the 0.3wt% cell 5 DMSO/EMImAC samples prepared via the 1 vial method and via the 3 vial method. With both types of samples, the DMSO was added to the vial containing the cellulose and then stirred for 3 minutes. After the cellulose was dispersed in the DMSO, the EMImAC was added and the solution was stirred again for 5 minutes. None of the DMSO samples were annealed or stored in the oven before testing, though they were allowed to homogenize overnight at room temperature. Interestingly, the samples containing DMSO exhibited the opposite behavior of those not containing DMSO. As depicted in figure 9, the samples containing DMSO prepared by the 1 vial method had slightly higher intrinsic viscosities than those prepared by the 3 vial method. This

may be due to the phase separation of DMSO, EMImAC, and cellulose, due to the magnetic stirring not fully mixing the entire 12mL. However, more studies are needed to determine the exact root of this behavior.

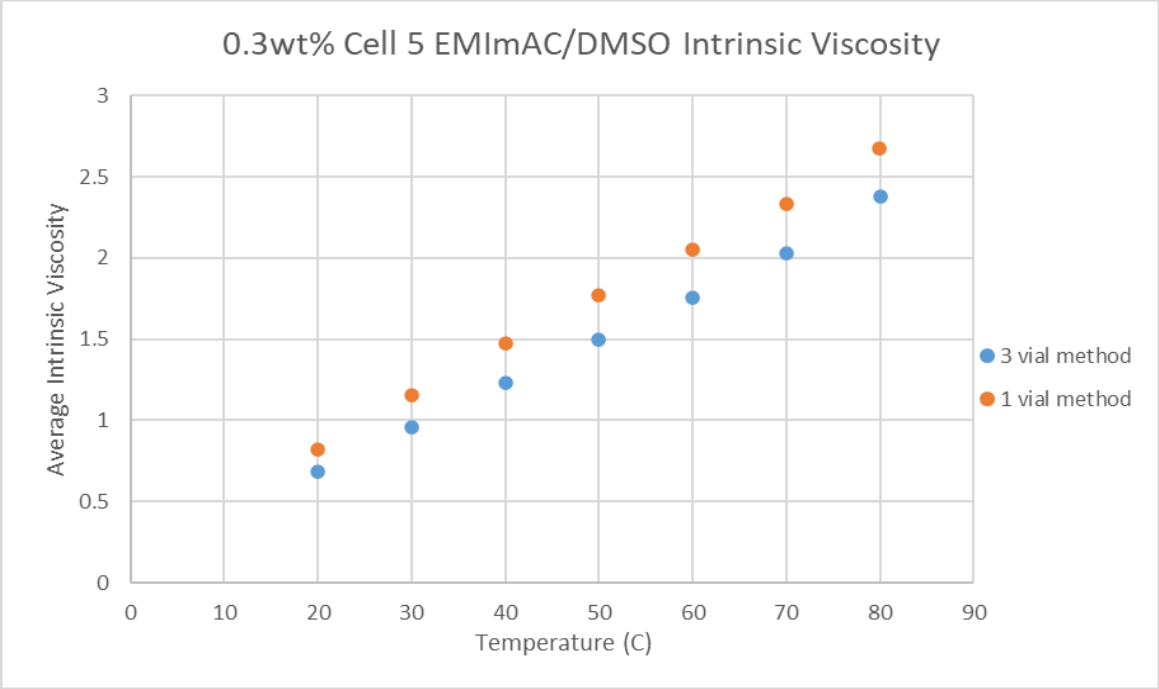

Figure 9: Comparison of the intrinsic viscosities of samples prepared via the 3 vial method (blue) with the 1 vial method (orange) for 0.3wt% cellulose samples containing DMSO

Additionally, unlike the cellulose/EMImAC samples not containing DMSO, the samples containing DMSO displayed intrinsic viscosities dependent on temperature in the intrinsic viscosity measurement. In order to verify this behavior, the same samples were then run in the interfacial rheometer for the same range of temperatures. This data, as seen in figures 10 and 11, does not indicate that the DMSO-containing samples exhibited a temperature dependence of viscosity. The behavior of the DMSO-containing samples in the capillary rheometer may be due

to the "blank" solvent used for comparison. The capillary rheometer, as discussed in the previous section, does not measure the sample's true viscosity, but rather its viscosity relative to a blank solvent. The blank used for all tests in this study was 12mL of pure EMImAC. Perhaps if the samples containing DMSO were run against a blank of DMSO/EMImAC, no temperature dependence would appear. This will be discussed further in the following sections. Also of note is that at both temperatures tested, 80°C and 20°C, the 3 vial sample preparation method had a higher complex viscosity than the 1 vial sample preparation method. This may be due to the fact that both samples were tested in the interfacial rheometer after completing a run in the capillary viscometer, which thoroughly mixes the sample during uptake. Additionally, the samples were heated to 80°C in the capillary viscometer and annealed at 80°C for 20 minutes in the rheometer before testing occurred. This may have helped homogenize the sample and increase cellulose dissolution, thus increasing the viscosities.

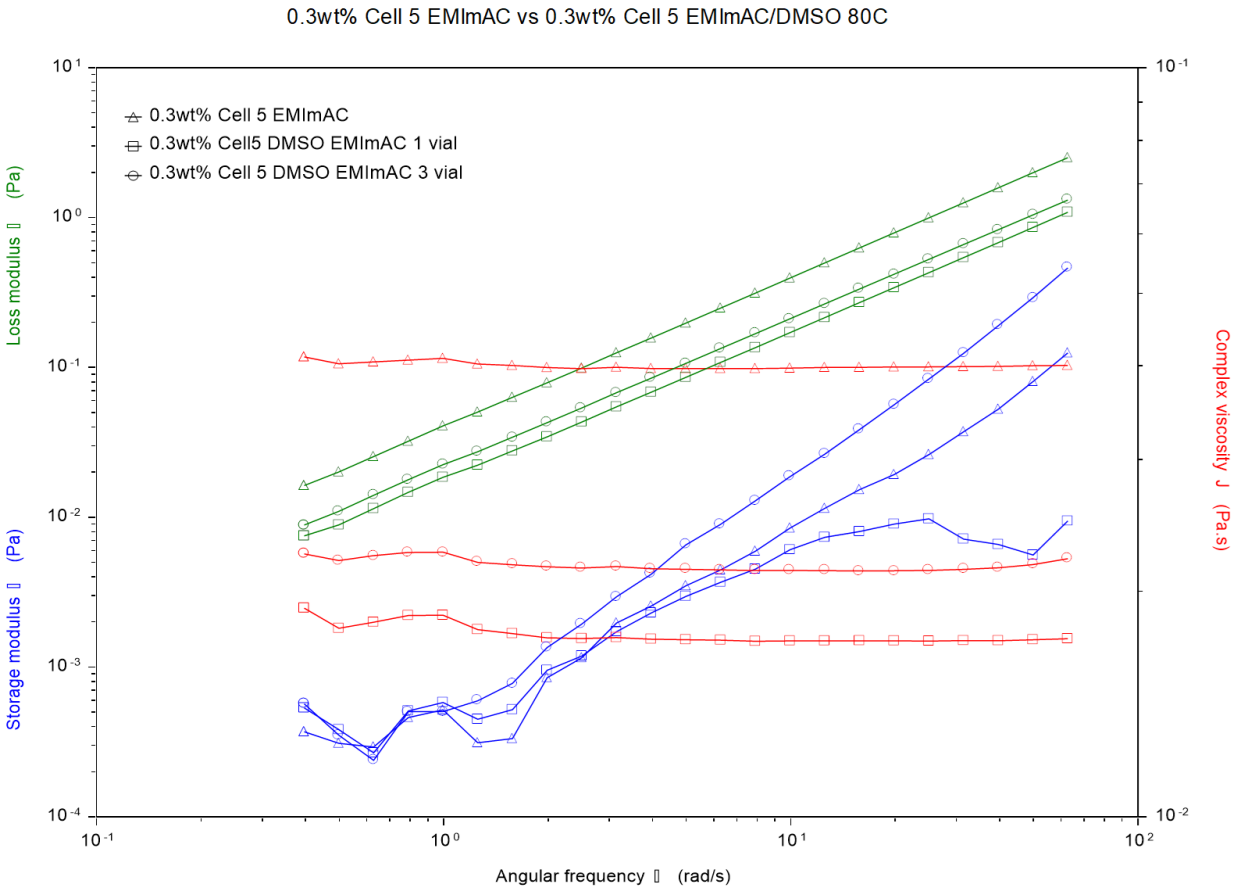

Figure 10: Comparison of the complex viscosities and moduli of samples prepared via the 3 vial method (red circles, middle line) with the 1 vial method (red squares, bottom line) for 0.3wt% cellulose samples containing DMSO at 80°C

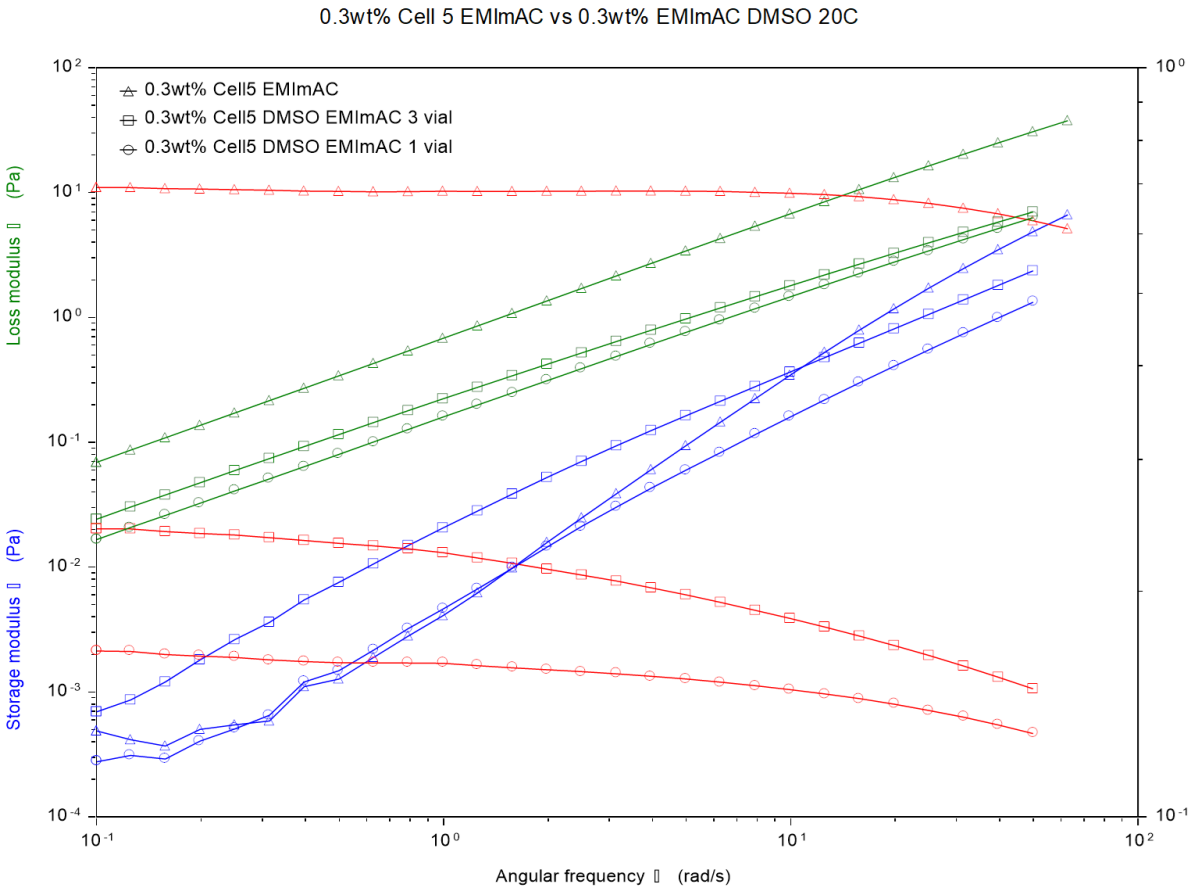

Figure 11: Comparison of the complex viscosities and moduli of samples prepared via the 3 vial method (red squares, middle line) with the 1 vial method (red circles, bottom line) for 0.3wt% cellulose samples containing DMSO at 20°C

Due to the results of both the intrinsic viscosity measurements with the capillary rheometer and the complex viscosity measurements with the interfacial rheometer, it was determined that both the samples containing DMSO and the samples without DMSO would be created via the 3 vial method to ensure homogeneity and uniform cellulose dissolution. Due to the concerns outlined above, all samples were first run in the capillary viscometer and then the interfacial rheometer to eliminate the potential for any extraneous influence on the samples.

Chapter 6

Experimental Procedures

Viscometry Measurements

All viscometry measurements were conducted on the Mini Automated Capillary Viscometer (mini-AV), which was obtained from the Cannon Instrument Company (State College, PA). The radius of the viscometer's Ubbelohde tube is 1.5 mm. The viscometer is located in a humidity-controlled chamber set at less than 5% RH in order to minimize contamination of the sample with water. The Ubbelohde tube in the mini-AV is submerged in silicone oil to regulate the temperature of the samples, and the sample stage is held at 80°C to anneal the sample and eliminate any residual water. The viscosity of each sample was calculated by measuring the flow time of each sample through the viscometer at a set temperature. Each test was run at least three times at each temperature, and any run time outside of the 0.5% standard error was repeated for a maximum total of six runs. The experiment began at 80° and decreased by 10°C after at least three runs were completed, with the final temperature being 20°C.

Rheology Measurements

The rheometer used in this experiment was the Discovery Hybrid Rheometer 3 (DHR-3) , obtained from TA Instruments (New Castle, DE). The rheometer was equipped with a stainless-steel cone and plate geometry of 60 mm diameter with a 1° angle and a truncation gap of 18 μm. A Peltier plate system was utilized to control the temperature of the bottom plate. All measurements were conducted with a nitrogen cap in order to prevent water contamination. The

nitrogen cap provided dry N_2 with <2ppm moisture at a flow rate between 80-100 mL/min. All samples were annealed at 80°C for 20 minutes before any measurements occurred in order to ensure homogeneity and eliminate residual moisture in the sample.

Chapter 7

Results and Discussion

Due to their importance in determining the properties of polymer solutions in relation to fiber-spinning and processing, this Thesis will employ both shear rheological characterization and solution viscometry to understand the behavior of cellulose/EMImAC and cellulose/EMImAC/DMSO solutions.

Solution Viscometry

In order to understand and to analyze the effect of cosolvent addition on the rheological behavior of the cellulose/EMImAC and the cellulose/EMImAC/DMSO solutions, the intrinsic viscosities of solutions containing 0.05wt%, 0.1wt%, 0.2wt%, and 0.3wt% cellulose in EMImAC were determined through the capillary viscometry method discussed in the Theoretical Background. Though the data collected on these samples was intended to be compared with that of solutions containing 0.05wt%, 0.1wt%, 0.2wt%, and 0.3wt% cellulose in a solvent mixture containing 50% DMSO and 50% EMImAC, the capillary viscometer was unable to accurately identify and measure the viscosities of the solutions below 0.3wt%. Thus, while a Huggins and Kraemer plot was obtained for the solutions not containing DMSO, one was unable to be created for the solutions containing DMSO. However, the intrinsic viscosity of the 0.3wt% cellulose solution in 50% DMSO/50% EMImAC and was compared to that of the 0.3wt% cellulose/EMImAC sample. Additionally, the two methods of sample preparation were compared.

Solutions without DMSO

The intrinsic viscosities of the 0.3wt%, 0.2wt%, 0.1wt% and 0.05wt% cellulose/ EMImAC samples were evaluated at 80°C and 20°C through the creation of a Huggins and Kraemer plot at both temperatures. The capillary viscometer measures the flow time of a sample and compares it to that of a blank solvent, in this case pure EMImAC with no cellulose added. The ratio of the flow time is reported by the viscometer as the relative viscosity η_r and is listed in table 3 for 80°C and table 5 for 20°C. Using the equations and definitions in Table 2 of the Theoretical Background chapter, the relative viscosity was used to calculate the reduced and inherent viscosities of each sample concentration. These values were then plotted against concentration in figure 12 as the Huggins and Kramer plots at each temperature.

Table 4: Viscometry Data and Viscosity Calculations for Cell 5 EMImAC Solutions at 80°C

Concentration c (g/dL)	Relative Viscosity η_r (t / t_0)	Specific Viscosity η_{sp} ($\eta_r - 1$)	Reduced Viscosity η_{red} (η_{sp} / c)	$\ln(\eta_r)$	Inherent Viscosity η_{inh} $\ln(\eta_r)/c$
0.3	4.444	3.444	11.481	1.492	4.972
0.2	2.573	1.573	7.863	0.945	4.725
0.1	1.486	0.486	4.859	0.396	3.960
0.05	1.113	0.113	2.268	0.107	2.148

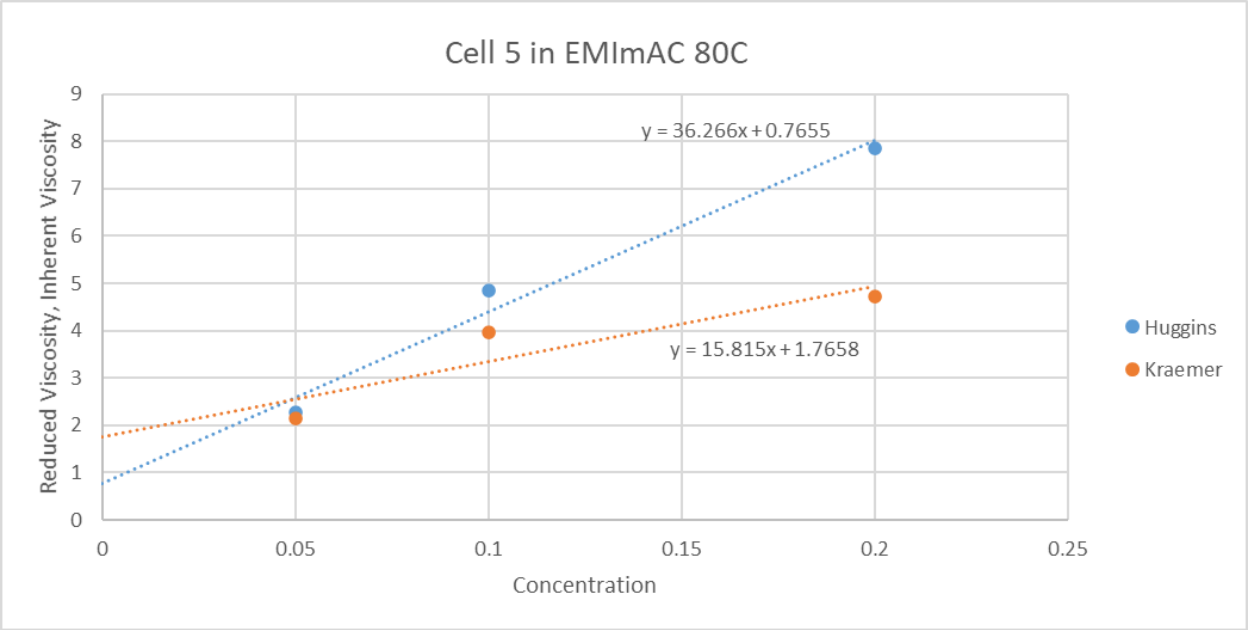

Figure 12: Huggins and Kraemer plot of cellulose/EMImAC samples at 80C

Figure 12 depicts the Huggins and Kraemer plots obtained for the 0.05wt%-0.2wt% cellulose solutions unmodified by the addition of DMSO. The specific viscosity of the 0.3wt% solution is 3.44, which is much greater than 1, and thus it was concluded that this concentration was above the overlap concentration c* such that the solution was no longer dilute. As the calculations for the Huggins and Kraemer plots are only valid for dilute solutions, the viscosities of the 0.3wt% solution were excluded. In order to calculate the intrinsic viscosity, both the reduced viscosity η_{red} (denoted as the Huggins series in the plot) and the inherent viscosity η_{inh} (denoted as the Kraemer series) were linearly fitted and extrapolated to a concentration of 0, the y-intercept. As noted in the Theoretical Background chapter, the y-intercept value of both the Huggins and Kraemer series represents the intrinsic viscosity [η]. Ideally, both y-intercepts have the same value. However, as made apparent in both plots, the extrapolated y-intercepts do not agree, and thus the intrinsic viscosity was calculated as the average of both values. The

calculated intrinsic viscosity of the cellulose/EMImAC solutions at 80°C was determined to be 1.26 dL/g and is reported in table 4 above.

The Huggins and Kraemer plot of the 0.2-0.05wt% cellulose/EMImAC solutions was also used to determine the Huggins and Kramer coefficients (k_H and k_K, respectively). The Huggins coefficient, as explained in the Theoretical Background section, is used to indicate the solvent's compatibility with the solute, and usually has a value of 0.3 for good solvents and 0.5 for poor solvents. Rewriting Eq. 16 gives the equation for the Huggins coefficient as $k_H = \frac{\eta_{sp}}{c\,[\eta]^2}$, where $\frac{\eta_{sp}}{c}$ is the slope of the Huggins plot and $[\eta]^2$ is the square of the y-intercept. The Huggins coefficient for the data set was calculated and is reported in table 3. The calculated value of the Huggins coefficient was calculated as $k_H = 61.88$, which is much greater than the accepted values between 0.3 and 0.5. This may be due to the use of only three data points to create a line of best fit. In order to accurately evaluate the compatibility of EMImAC with cellulose and to determine the efficacy of EMImAC as a solvent for cellulose, it is strongly recommended that the measurements be rerun with samples of a broader range of concentrations to ensure that the flow times and reduced viscosities correctly represent the system.

The Kraemer coefficient for both data sets including and excluding the results of the 0.05wt% cellulose/EMImAC sample were also determined. Rewriting Eq. 17 in the Theoretical Background chapter yields the equation $k_K = \frac{ln(\eta_r)}{c\,[\eta]^2}$, where $\frac{ln(\eta_r)}{c}$ is the slope of the Kraemer plot and $[\eta]^2$ is the square of the y-intercept. Using the equations of the linear lines of best fit for each Kraemer series, the k_K was determined to be 5.07. This value is also listed below in table 5. As noted in the Theoretical Background, the Kraemer coefficient is usually either a negative value or zero, as it can also be obtained by subtracting ½ from the Huggins coefficient. Both methods

of calculating the Kraemer coefficient are included in table 5. Due to the anomalously high values of the Huggins coefficient, the k_K as determined from the plot and the k_K as determined by subtracting ½ from k_H do not agree. It is assumed that the value obtained from the plot is more accurate, as it is closer to the expected value of the Kraemer coefficients, though further testing is needed. It is highly recommended that the experiments be completed again, perhaps with new samples or after recalibrating the capillary viscometer, such that more accurate data can be obtained.

Table 5: Average Intrinsic Viscosity and Huggins and Kraemer Coefficients for Cell 5 EMImAC Solutions at 80°C

Huggins and Kraemer Plot	Average Intrinsic Viscosity (dL/g)	$k_H = \frac{\eta_{sp}}{c\,[\eta]^2}$	$k_K = \frac{ln(\eta_r)}{c\,[\eta]^2}$	$k_K = k_H - \frac{1}{2}$
Cell 5 EMImAC 80°C	1.26	61.9	5.07	61.4

The same process of calculations described above was utilized for the data obtained at 20°C for the 0.2wt%, 0.1wt%, and 0.05wt% cellulose/EMImAC solutions. Similar to the results of the test at 80°C, the specific viscosity of the 0.3wt% solution is much greater than 1, and the viscosities of the 0.3wt% solution were excluded from the Huggins and Kraemer plot. The relative viscosities of each sample was determined by the capillary rheometer and then used to calculate the subsequent viscosities until the reduced viscosity η_{red} and the inherent viscosity η_{inh} were obtained. These values were then used to create figure 13, the Huggins and Kraemer plot for the cellulose/EMImAC system at 20°C. The inherent viscosity was plotted against concentration as the Kraemer series in figure 13, and the reduced viscosity was plotted against concentration as the Huggins series in figure 13.

Table 6: Viscometry Data and Viscosity Calculations for Cell 5 EMImAC Solutions at 20°C

Concentration c (g/dL)	Relative Viscosity η_r (t / t_0)	Specific Viscosity η_{sp} ($\eta_r - 1$)	Reduced Viscosity η_{red} (η_{sp} / c) (dL/g)	$\ln(\eta_r)$	Inherent Viscosity η_{inh} $\ln(\eta_r)/c$ (dL/g)
0.3	3.992	2.992	9.972	1.384	4.614
0.2	2.725	1.725	8.627	1.003	5.013
0.1	1.590	0.590	5.899	0.464	4.637
0.05	1.286	0.286	5.730	0.252	5.039

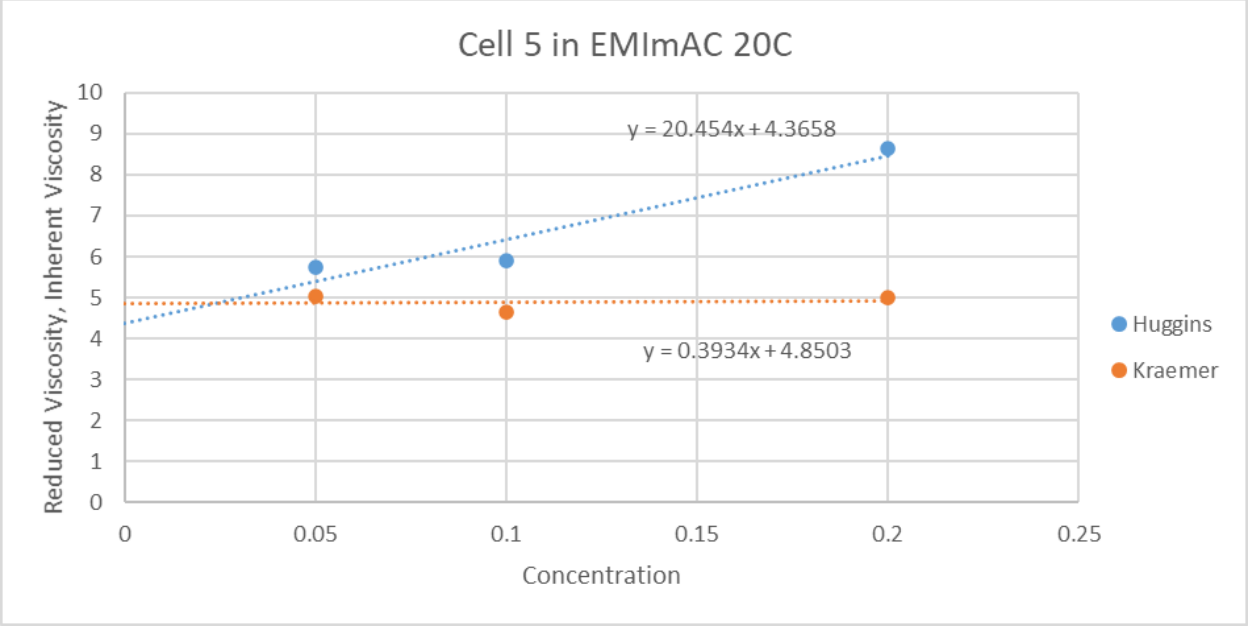

Figure 13: Huggins and Kraemer plot of cellulose/EMImAC at 20C

Although not the same value, the y-intercepts of the Huggins and Kraemer series were much closer than those calculated using the data from the 80°C experiment. The average intrinsic viscosity of the system at this temperature, calculated by averaging both extrapolated y-

intercepts, was determined to be 4.61 dL/g. The Huggins and Kraemer plots and the equations of the lines of best fit were also calculated in the same manner as discussed above. The Huggins coefficient k_H was determined through the rearranged equation $k_H = \frac{\eta_{sp}}{c\,[\eta]^2}$, where $\frac{\eta_{sp}}{c}$ is the slope of the Huggins plot and $[\eta]^2$ is the square of the y-intercept. This value was calculated as 1.07. The Kraemer coefficient k_K was calculated in two ways: first by using the equation $k_K = \frac{ln(\eta_r)}{c\,[\eta]^2}$, where $\frac{ln(\eta_r)}{c}$ is the slope of the Kraemer plot and $[\eta]^2$ is the square of the y-intercept, and then by using the equation $k_K = k_H - \frac{1}{2}$. The calculated values of k_K were 0.017 and 0.57, respectively, and are listed below in table 7. The values for both the Huggins and Kraemer coefficients were much closer to the acceptable range for the cellulose/EMImAC system at 20°C than at 80°C.

Table 7: Average Intrinsic Viscosity and Huggins and Kraemer Coefficients for Cell 5 EMImAC Solutions at 20°C

Huggins and Kraemer Plot	**Average Intrinsic Viscosity (dL/g)**	$\boldsymbol{k_H = \frac{\eta_{sp}}{c\,[\eta]^2}}$	$\boldsymbol{k_K = \frac{ln(\eta_r)}{c\,[\eta]^2}}$	$\boldsymbol{k_K = k_H - \frac{1}{2}}$
Cell 5 EMImAC 20°C	4.61	1.07	0.017	0.57

As anticipated, the cellulose/EMImAC solutions were much less viscous at higher temperatures than lower temperatures; the intrinsic viscosity of the system at 80°C was between 1.26 dL/g, while the intrinsic viscosity of the system at 20°C was nearly four times that value (4.61). However, the data for both temperatures resulted in Huggins and Kraemer coefficients outside of the expected values, indicating that perhaps the data is unreliable and does not give an accurate assessment of the intrinsic viscosity of the system.

Solutions with DMSO

The same process was repeated for the 0.05wt%, 0.1wt%. 0.2wt%, and 0.3wt% cellulose solutions containing a solvent mixture of 50% DMSO and 50% EMImAC, but the measurements were unsuccessful. The capillary viscometer was unable to detect the solutions with a concentration below 0.3wt%, perhaps due to their extremely dilute nature, so no data was obtained for the smallest three samples. Without at least four data points, the Huggins and Kraemer plot could not be created, and the coefficients and intrinsic viscosity could not be determined. As noted above, the solutions without DMSO were not dilute enough to be considered in a Huggins and Kraemer plot. However, these values were still included in figure 4 to highlight the effect of DMSO. Figure 14 graphs the relative viscosity data of four different 0.3wt% solutions were compared from 20-80°C. Two samples were made with 100% EMImAC as the solvent, and two were made with a solvent mixture of 50% DMSO and 50% EMImAC. One of each sample per solution type was made via the 1 vial method and one was prepared according to the 3 vial method. Both methods of sample preparation are described in detail in the previous chapter.

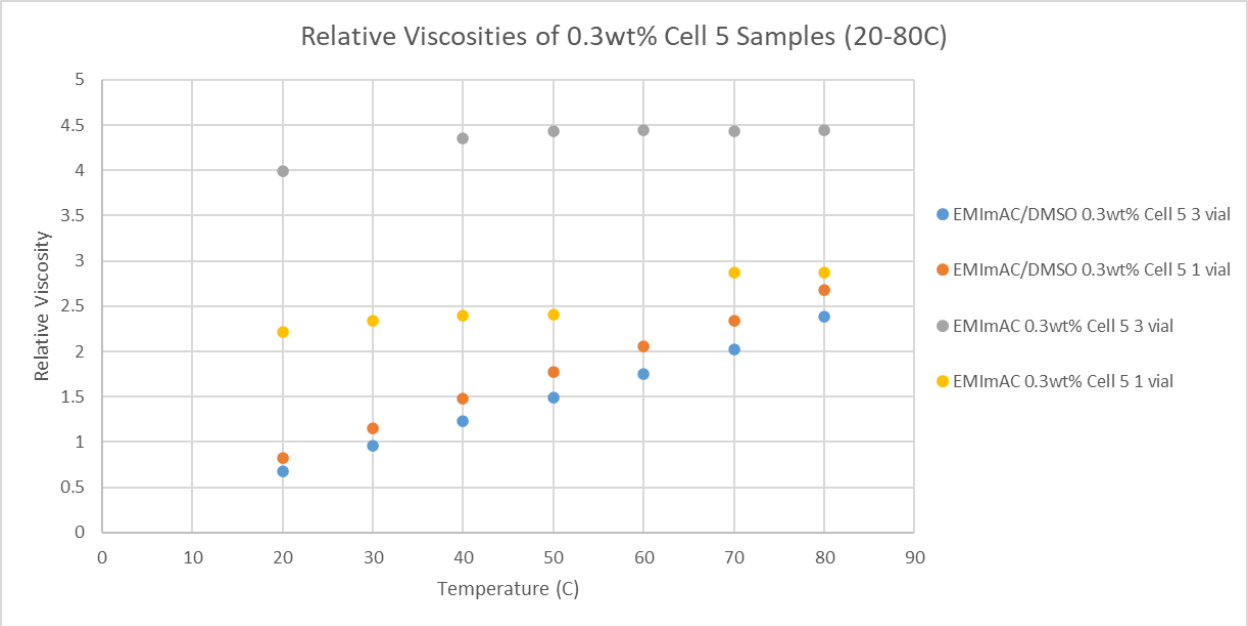

Figure 14: Comparison of the Relative Viscosities of 0.3wt% cellulose samples in EMImAC (gray, yellow) and in 50% EMImAC/50% DMSO (blue, orange)

As noted in the Sample Preparation section, both methods of sample preparation yielded different relative viscosities. The 3 vial method produced a sample with higher relative viscosity for the solutions without DMSO, while the opposite was true for the solutions containing the cosolvent. The viscosities of the samples made with DMSO also show a much greater dependence on temperature than the viscosities of the samples made with pure EMImAC solvent. This anomaly was discussed in the Sample Preparation section, and was suggested to result from the use of a pure EMImAC sample as the reference solution. However, the strong temperature dependence of the EMImAC/DMSO solutions indicates that the solvent quality improves with increasing temperature, which is not true for ionic liquid-based system.

Though the intrinsic viscosity of the cellulose/EMImAC system could not be compared to the intrinsic viscosity of the system containing DMSO, the preliminary data from the measurement of the relative viscosity of 0.3wt% cellulose in 50% DMSO and 50% EMImAC

supports the initial hypothesis that the addition of DMSO reduces the viscosity of the cellulose/EMImAC solutions. The 0.3wt% cellulose/ EMImAC solution prepared by the three vial method, which was determined to be more accurate due to the dispersion of concentration gradients within the sample, was significantly higher than both solutions containing DMSO. Even at the highest temperature where the relative viscosities were the closest, the samples with DMSO were almost 2 dL/g smaller than the solution without DMSO, enough that the solution was reclassified into the dilute regime. More tests are needed to confirm these results, especially due to the lack of viable data for the 0.2wt%, 0.1wt%, and 0.05wt% solutions with DMSO.

Shear Rheology

The rheological behavior of the 0.05-0.3wt% cellulose solutions in EMImAC and 50% EMImAC/50% DMSO were analyzed at 20°C and 80°C through a series of frequency sweep measurements. All samples were annealed as described in the Experimental Procedures section before any tests were conducted. The frequency sweeps were conducted at the same strain of 10% over the same frequency range for every sample. As discussed in the Theoretical Background, the rheometer measures the phase angle δ and the magnitude of the complex modulus $|G^*| = G_d$. The TRIOs software in the rheometer then calculates the storage modulus G', loss modulus G", and complex viscosity η^* that are graphed over the frequency range in the plots

Solutions without DMSO

The results of the frequency sweeps at 80°C and 20°C for the 0.05wt%, 0.1wt%, 0.2wt%, and 0.3wt% cellulose samples in EMImAC are shown below. Figures 15 and 16 are the

frequency sweeps of the 0.05wt% sample at 80°C and 20°C, respectively. As apparent in both the 80°C and 20°C, the 0.05wt% cellulose solution is characterized by predominantly liquid-like behavior. The sample appears to reach the terminal regime of a viscoelastic liquid, as the loss modulus G" (green) dominates over the storage modulus G' (blue) at both temperatures. Similar to the intrinsic viscosity determinations for the same samples, the complex viscosity (red) is larger at lower temperatures for frequencies between 10^2 and 10^0 rad/s.

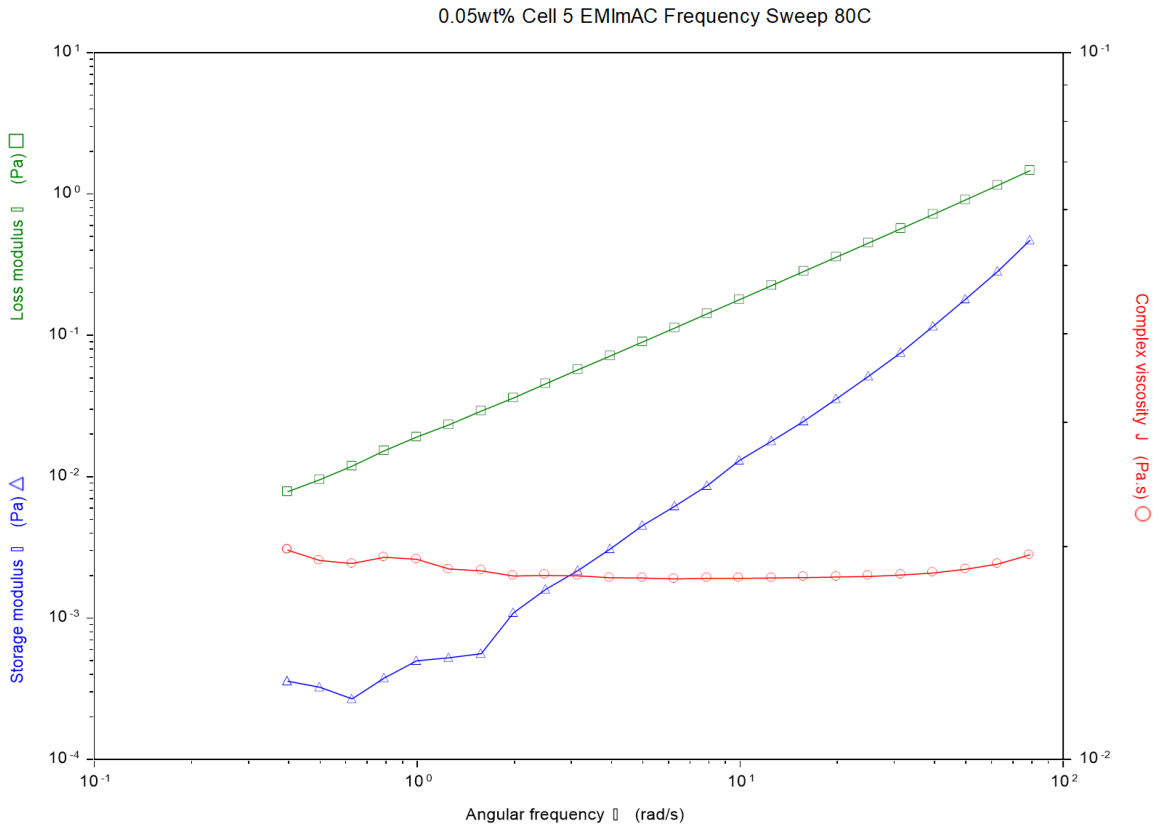

Figure 15: Frequency sweep of 0.05wt% cellulose in EMImAC at 80°C

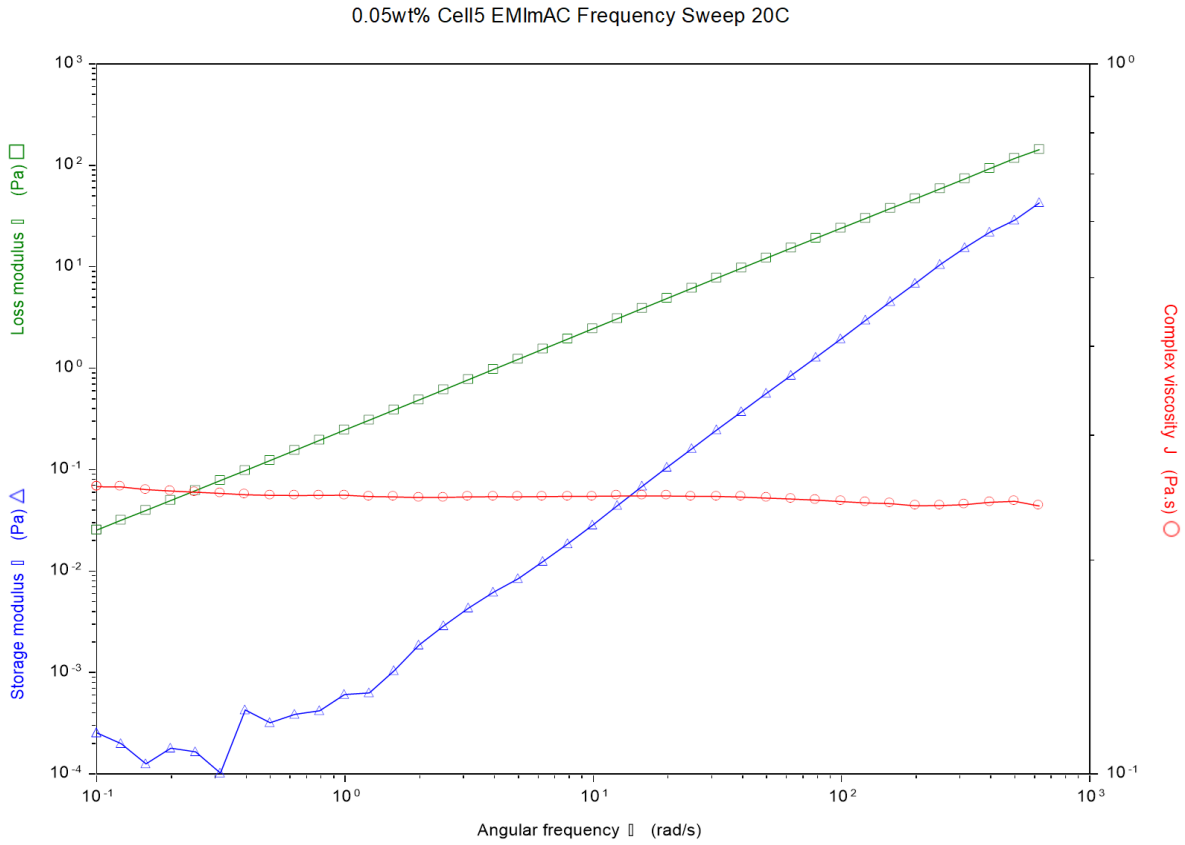

Figure 16: Frequency sweep of 0.05wt% cellulose in EMImAC at 20 °C

Similar behavior is seen for the 0.1wt% cellulose sample. The frequency sweeps of the 0.1wt% sample at 80°C and 20°C are represented in figures 17 and 18. The 0.1wt% cellulose solution also reaches the terminal regime of a viscoelastic liquid at both temperatures. Over the entire frequency spectrum, the loss modulus G" (green) is much greater than the storage modulus G' (blue) at 80°C and 20°C. The complex viscosity (red) is approximately two orders of magnitude larger at the lower temperatures for frequencies between 10^2 and 10^0 rad/s. The complex viscosity does not show a dependence on frequency.

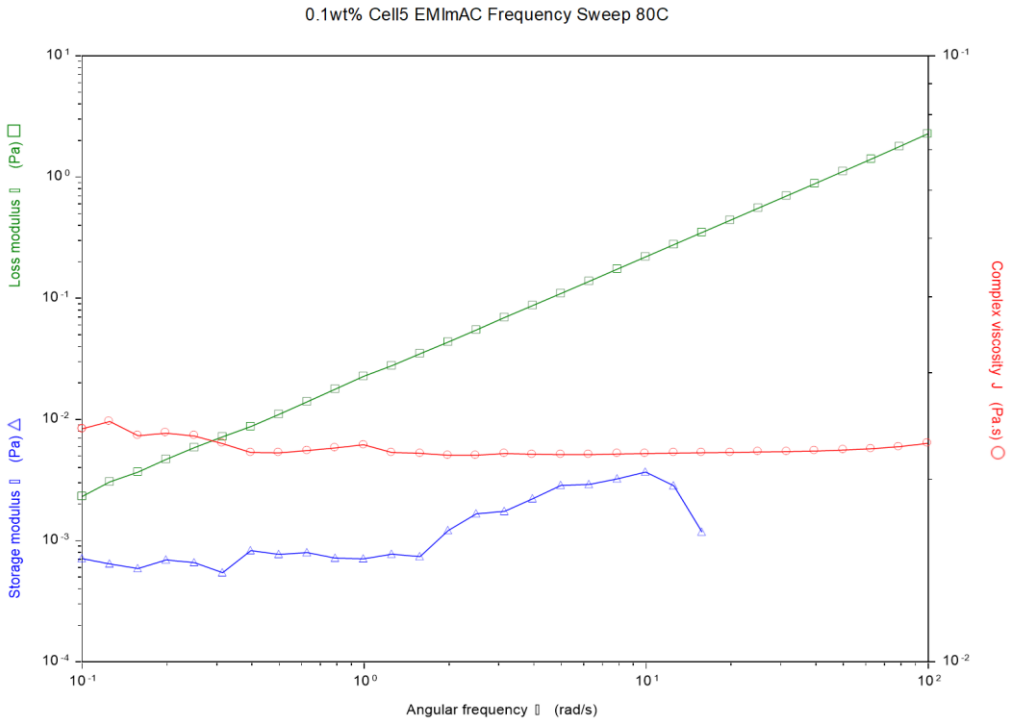

Figure 17: Frequency sweep of 0.1wt% cellulose in EMImAC at 80°C

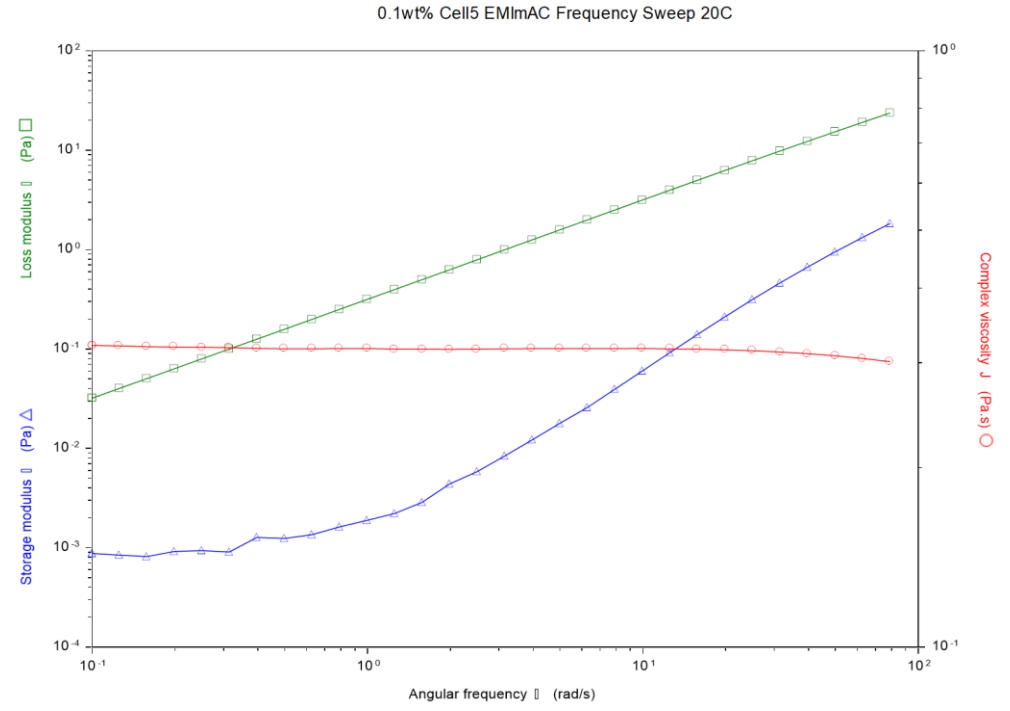

Figure 18: Frequency sweep of 0.1wt% cellulose in EMImAC at 20°C

The next two graphs, figures 19 and 20, depict the frequency sweeps for the 0.2wt% cellulose sample at 80°C and 20°C, respectively. In comparison to the 0.05wt%, 0.1wt%, and 0.3wt% samples, the 0.2wt% sample displays anomalous behavior at 20°C. Unlike the same sample at 80°C, the 0.2wt% sample does not reach the terminal regime for a viscoelastic liquid at low frequencies. Instead, the storage modulus overtakes the loss modulus at a frequency of about 10^1 rad/s, which emulates the behavior of a viscoelastic liquid in the transition region. Additionally, the large G' indicates that the sample is responding elastically, which is associated with solid-like behavior. However, the frequency sweep at 80°C still represents liquid-like behavior. Due to the sample's response at 80°C as well as the frequency sweeps of the 0.3wt% sample at both temperatures, it cannot be definitively concluded that the 0.2wt% sample forms associations or becomes gel-like. Rather, the experiment should be repeated to confirm such behavior, and frequency sweeps should be conducted at temperatures between 80°C and 20°C to probe whether this was a spontaneous transition.

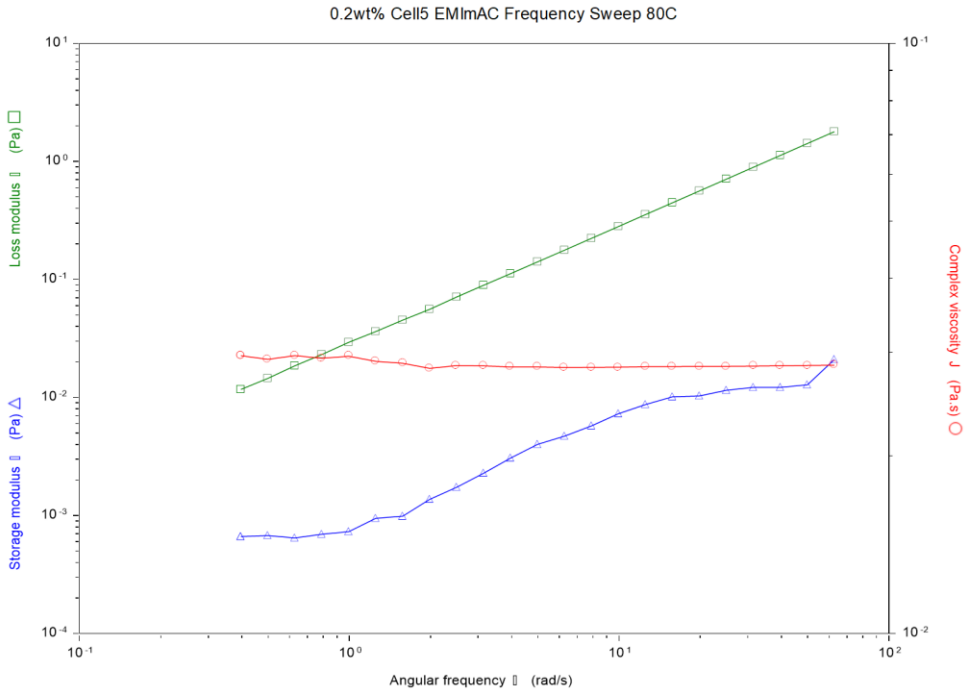

Figure 19: Frequency sweep of 0.2wt% cellulose in EMImAC at 80°C

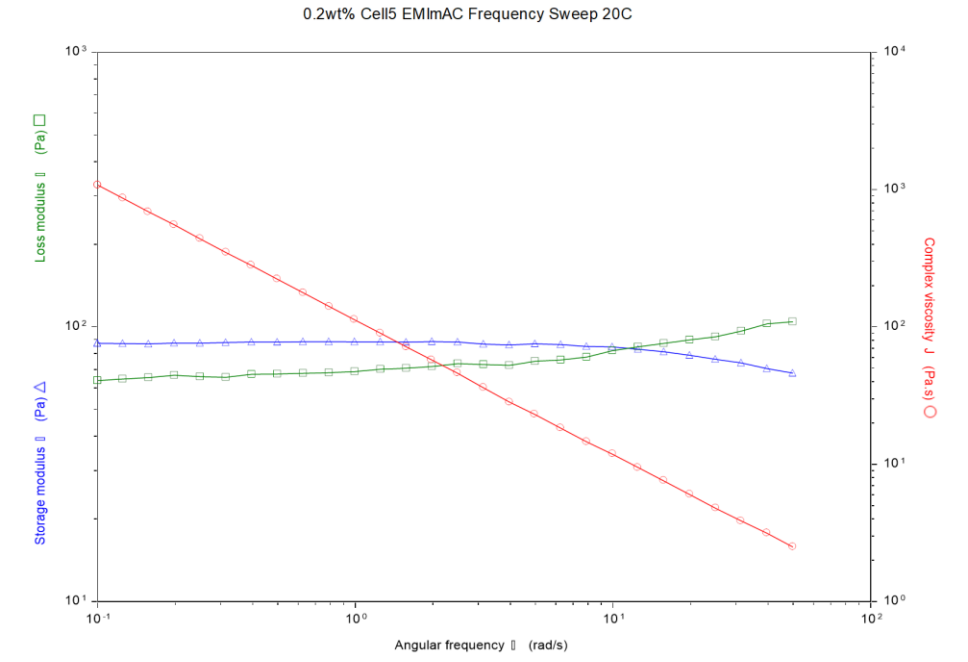

Figure 20: Frequency sweep of 0.2wt% cellulose in EMImAC at 20 °C

Figures 21 and 22 represent the frequency sweeps at 80°C and 20°C for the 0.3wt% cellulose samples in EMImAC. Despite the behavior of the 0.2wt% cellulose sample at 20°C, the 0.3wt% cellulose solution continues the trend established with the frequency sweeps of the 0.05wt% sample. At both temperatures, the 0.3wt% solution appeared to reach the terminal regime due to the dominance of the loss moduli. Though the true indication of the terminal regime is the loss modulus having a slope of 1 and the storage modulus having a slope of 2, the data begins to fluctuate at the low frequency range and slope cannot be determined with accuracy. However, the 0.3wt% solution returns to behaving as a liquid at both temperatures over the entire frequency range, though the complex viscosity is much higher at the lower temperature.

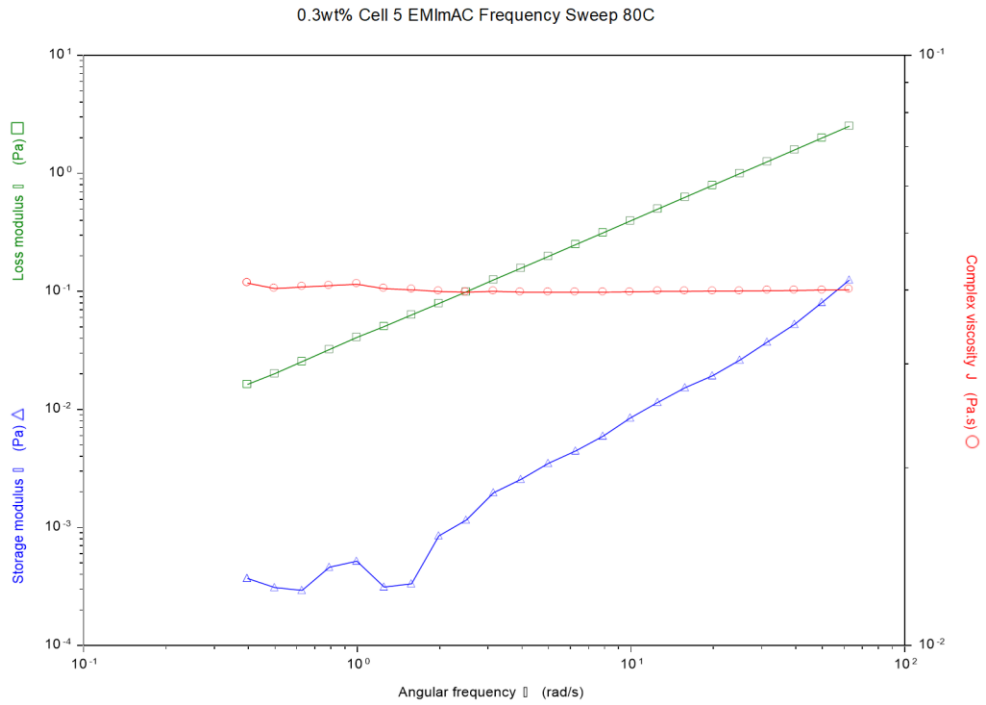

Figure 21 : Frequency sweep of 0.3wt% cellulose in EMImAC at 80°C

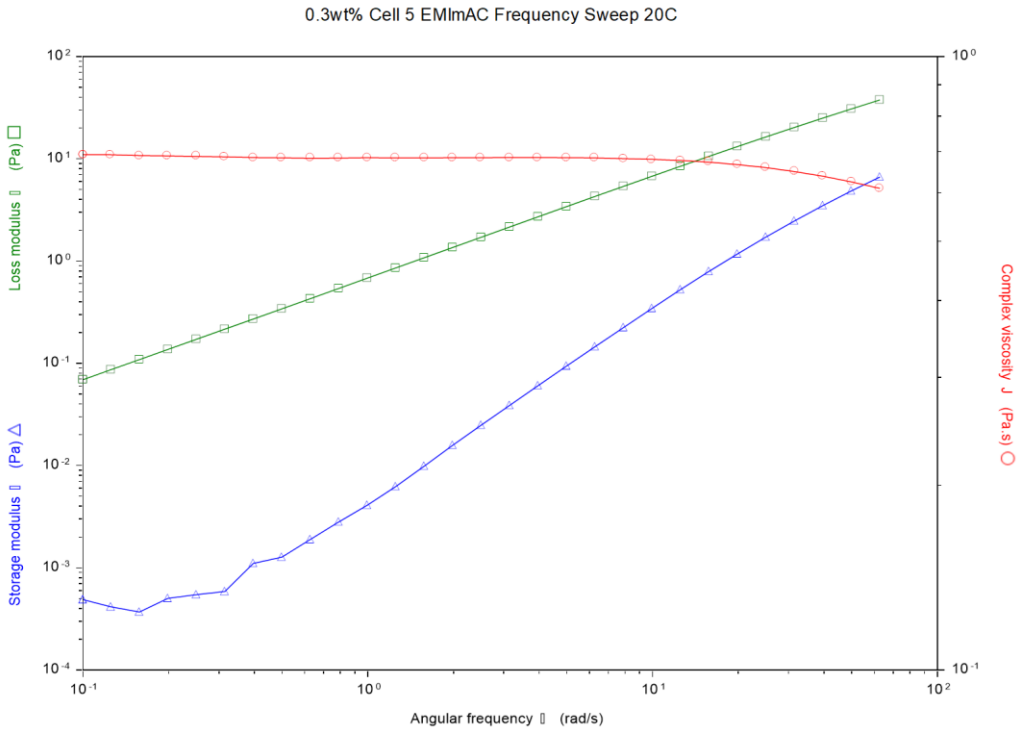

Figure 22: Frequency sweep of 0.3wt% cellulose in EMImAC at 20°C

The frequency sweeps of the 0.05wt%, 0.1wt%, 0.2wt% and 0.3wt% cellulose samples in EMImAC at 80°C are overlaid in figure 23, while the frequency sweeps of the 0.05wt%, 0.1wt%, and 0.3wt% cellulose samples in EMImAC at 20°C in figure 24. The 20°C frequency sweep of the 0.2wt% sample was excluded from the compilation in order to highlight the similarity in the rheological behavior of the other three solutions. The general trends identified previously are apparent in each figure, as the solutions appear to respond in a liquid-like manner throughout the range of frequencies. Also of note is that the complex viscosity steadily decreases with concentration. In Figure 9.1, the red circles represent the 0.3wt% solution, the red squares represent the 0.2wt% solution, the red triangles the 0.1wt% solution, and the red diamonds the 0.05wt%. All of the complex viscosities at this temperature appear to be independent of frequency.

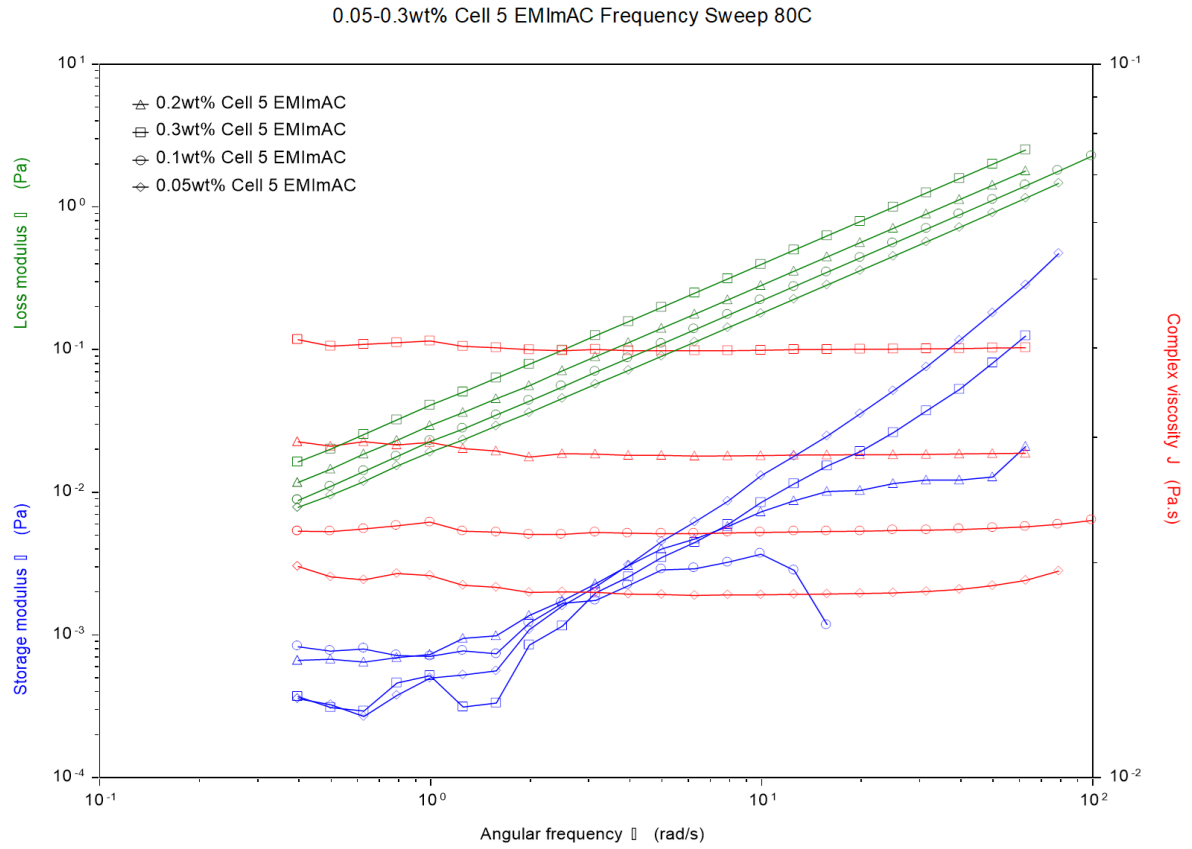

Figure 23: Frequency sweeps of the 0.3wt% solution (top, squares), 0.2wt% solution (triangles), 0.1wt% solution (circles), and 0.05wt% solution (bottom, diamonds) at 80°C

Much of the same trends seen at 80°C hold for the frequency sweeps at 20°C (figure 24). As noted above, the 0.2wt% sample was excluded from the overlay in figure 9.2. However, the 0.05wt%, 0.1wt%, and 0.3wt% solutions all display relatively consistent liquid-like behavior, and appear to be within the terminal region. The complex viscosity appears to decrease with concentration, which reflects the behavior seen at 80°C. The trend of the complex viscosity decreasing at high frequencies is also prevalent in the graph, and the solutions with higher concentrations show a greater drop. The viscosities of both the 0.1wt% cellulose and the 0.3wt% cellulose solution appear to start decreasing at the same frequency.

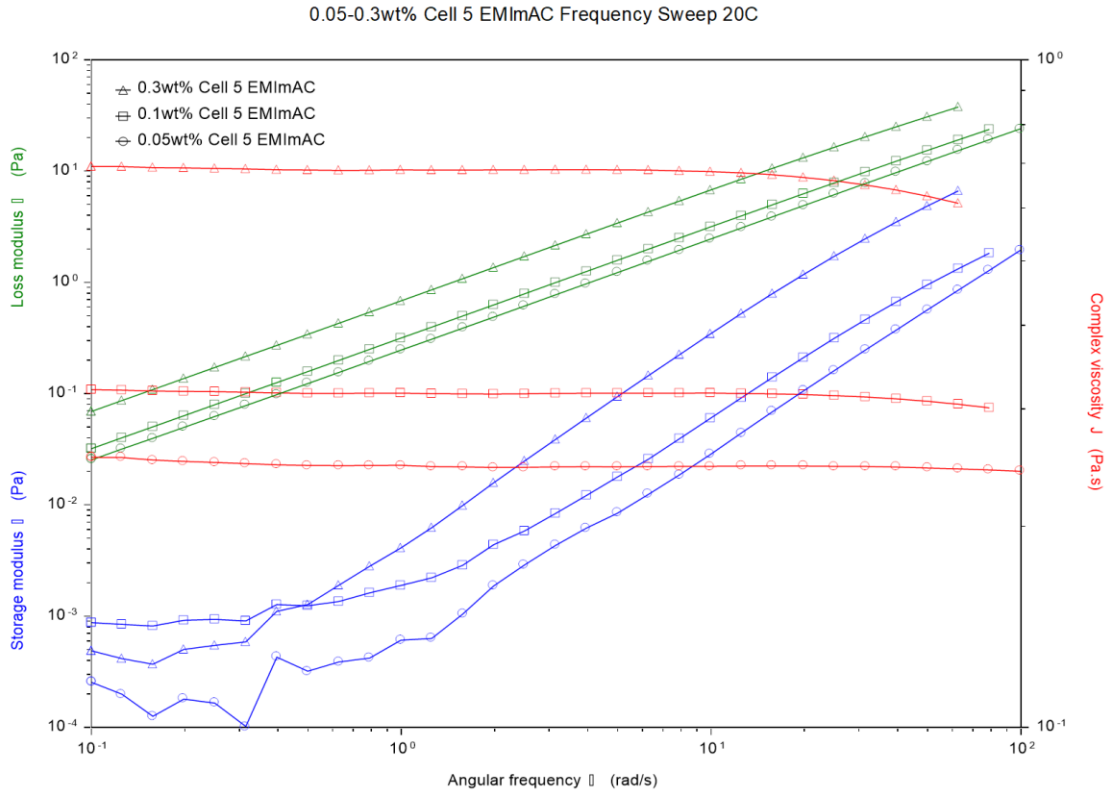

Figure 24: Frequency sweeps of the 0.3wt% solution (top, triangles), 0.1wt% solution (middle, squares), and 0.05wt% solution (bottom, circles) at 20°C

Solutions with DMSO

The same procedure was followed for conducting and evaluating the frequency sweeps for the solutions of 0.05wt%-0.3wt% cellulose in 50% EMImAC and 50% DMSO. For brevity, the frequency sweeps of the samples containing DMSO are not shown individually like that of the samples without DMSO, as the same general trends persist and no extraneous results were obtained like those of the 0.2wt% cellulose sample. Figure 25 depicts the overlay of the frequency sweeps of the 0.05wt%, 0.1wt%, and 0.2wt% cellulose solutions in 50% EMImAC/50% DMSO at 80°C. The frequency sweeps of the 0.3wt% cellulose in 50% EMImAC/50% DMSO samples prepared by the 1 vial method and the 3 vial method are also

included. Just like the samples without DMSO, every solution appeared to behave as a viscoelastic liquid that is approaching the terminal regime, as evidenced by the loss moduli dominating the storage moduli. Additionally, the complex viscosities remain relatively independent of frequency between roughly 10^0 and 10^2 rad/s, though the 0.05wt% and 0.1wt% samples have a dramatic increase in complex viscosity before 10^2 rad/s.

Interestingly, the 0.05wt% and 0.1wt% samples exhibit extremely similar curves, whereas the corresponding samples without DMSO do not. To the author's knowledge, this behavior has not been identified in other ionic liquid/DMSO/ cellulose solutions. One potential explanation could be that the DMSO only decreases the viscosity up to a certain extent. The cellulose concentration of both samples are extremely small, so the 50% DMSO may have completely solvated all of the cellulose. Though it may not be feasible or practical, an exploration into the rheological behavior of even smaller cellulose concentrations in EMImAC/DMSO systems could elucidate the mechanism behind this occurrence.

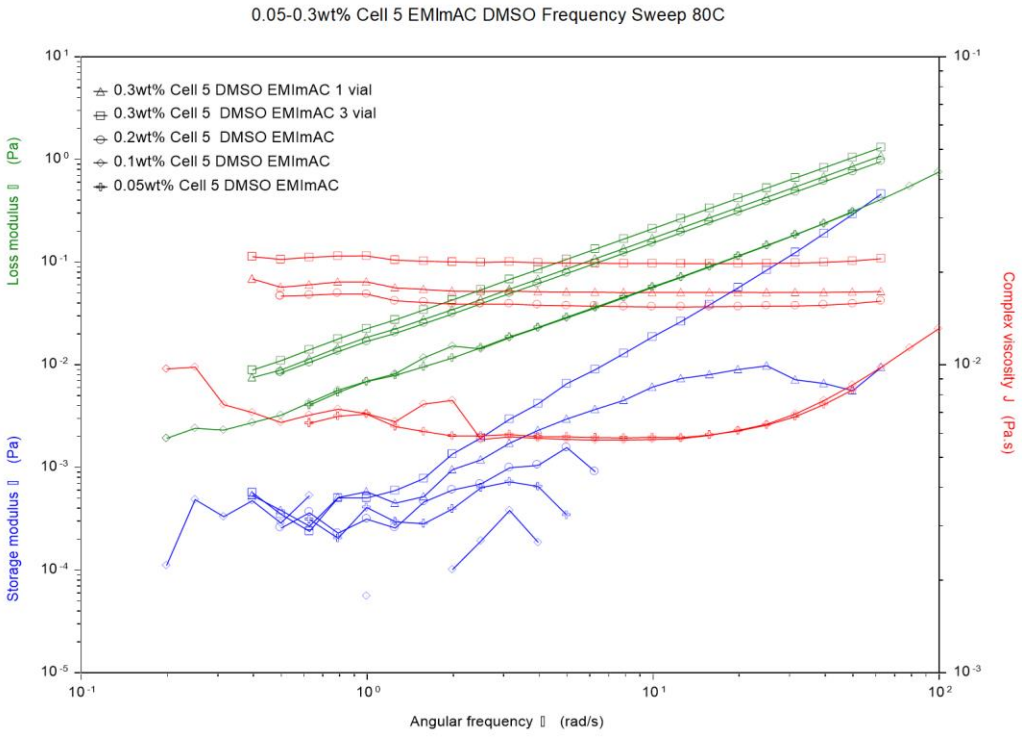

Figure 25: Overlay of frequency sweeps of 0.05wt%-0.3wt% cellulose in 50% EMImAC/50% DMSO at 80°C

Figure 26 depicts the overlay of the frequency sweeps of the 0.05wt%, 0.1wt%, and 0.2wt% cellulose solutions in 50% EMImAC/50% DMSO at 20°C. The frequency sweeps of the 0.3wt% cellulose in 50% EMImAC/50% DMSO samples prepared by the 1 vial method and the 3 vial method are also shown. Much like the samples of corresponding concentrations without DMSO, every solution displayed a predominantly liquid-like response, as the loss moduli were consistently larger than the storage moduli. The slopes of G" and G' appeared to approach 1 and 2 at low frequencies, respectively, which is characteristic of the terminal response of a viscoelastic liquid. This behavior is more prevalent at the higher concentrations, as the storage moduli of the concentrations below 0.2wt% are erratic and noisy. The complex viscosities remain relatively independent of frequency between roughly 10^0 and 10^2 rad/s, which reflects the

behavior of the samples without DMSO. The DMSO samples of higher concentrations also exhibit the decrease in complex viscosity at higher frequencies. However, unlike the samples without DMSO, the 0.05wt% and 0.1wt% cellulose samples in 50% EMImAC and 50% DMSO display a dramatic increase in complex viscosity after 10^2 rad/s.

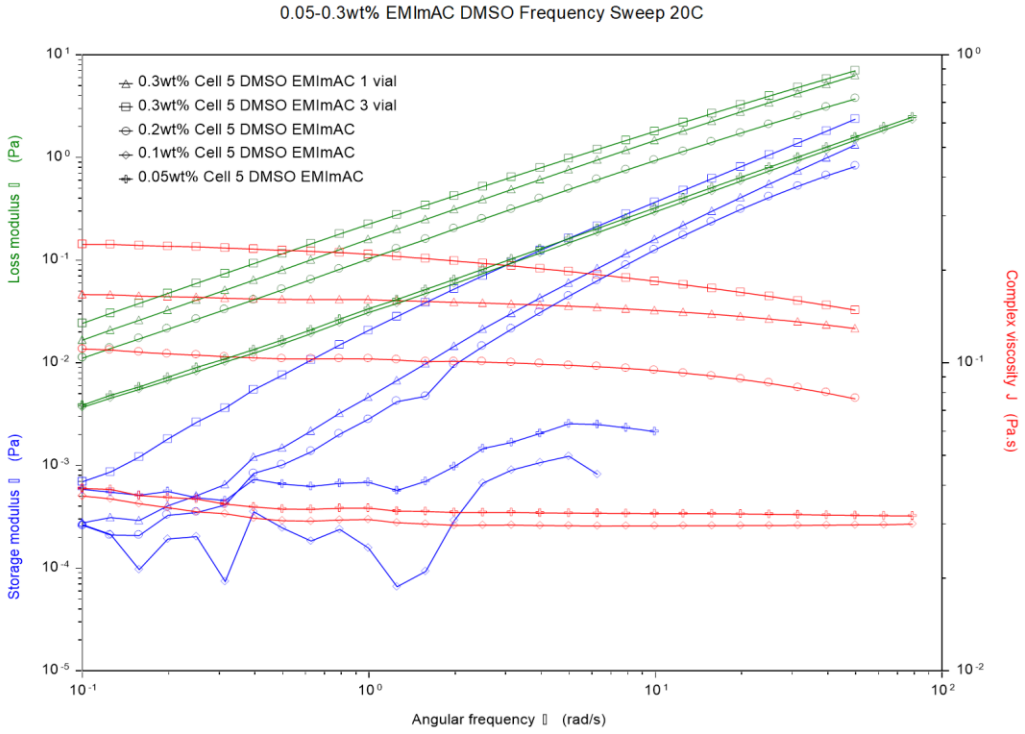

Figure 26: Overlay of frequency sweeps of 0.05wt%-0.3wt% cellulose in 50% EMImAC/50% DMSO at 20°C

Effect of DMSO Addition

The following figures compare the frequency sweeps of samples containing DMSO and samples without DMSO of the same concentration of cellulose in order to gauge the effect of DMSO on the rheological properties of the samples. Just as suggested by the investigations discussed in the Literature Review section, the addition of DMSO largely decreased the viscosity of the cellulose samples of every concentration by several orders of magnitude at both 80°C and

20°C. This may be due to the cosolvent effect of DMSO, which is proposed to increase the dissolution of cellulose by freeing the ions in the ionic liquid solvent.

Figures 27 and 28compare the frequency sweeps of the 0.05wt% cellulose solution in 100% EMImAC and the 0.05wt% cellulose solution in 50% EMImAC/50% DMSO at 80°C and 20°C, respectively. At 80°C and 20°C, both the sample containing DMSO and the sample without DMSO were characterized as liquid-like. The slopes of both loss moduli at 80°C and 20°C seem to reach 1, indicating a terminal response, but the slopes of the storage moduli are too noisy at the low frequency range to determine the slope. Most notable is the dramatic decrease in the complex viscosity of the solutions containing DMSO at both temperatures. Across the frequency spectrum, the DMSO-containing solution was two orders of magnitude smaller at 80°C and three orders of magnitude smaller at 20°C. Neither solution displays a temperature dependence of complex viscosity.

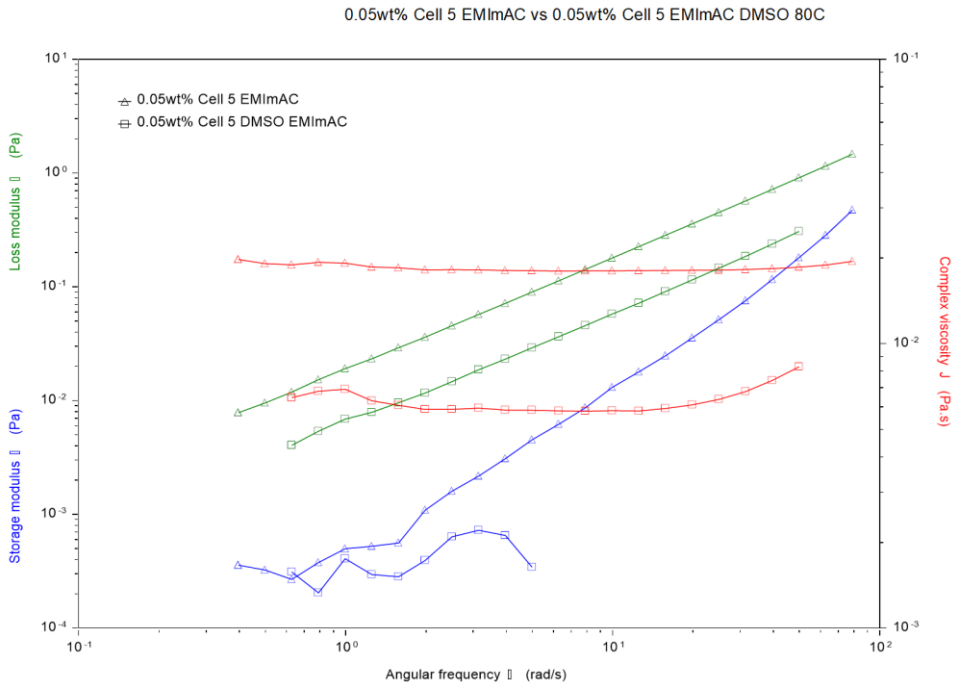

Figure 27: Frequency sweeps of 0.05wt% cellulose in 100% EMImAC (triangles, top) and 50% EMImAC/50% DMSO (squares, bottom) at 80°C

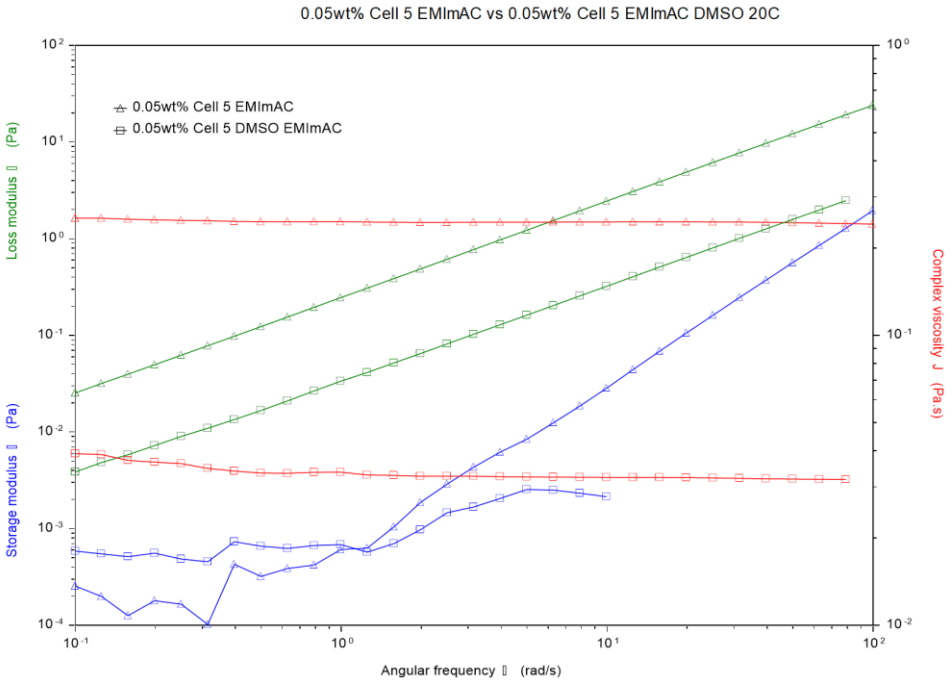

Figure 28: Frequency sweeps of 0.05wt% cellulose in 100% EMImAC (squares, top) and 50% EMImAC/50% DMSO (triangles, bottom) at 80°C

Figures 29 and 30 compare the frequency sweeps of the 0.1wt% cellulose solution in 100% EMImAC and the 0.1wt% cellulose solution in 50% EMImAC/50% DMSO at 80°C and 20°C, respectively. At 80°C and 20°C, both the sample containing DMSO and the sample without DMSO were characterized as liquid-like due to the loss modulus being larger than the storage modulus. However, the storage moduli of both samples at 80°C are noisy and do not extend into the higher frequencies. The slopes of both loss moduli at 80°C and 20°C seem to approach 1, indicating a terminal response, but the slopes of the storage moduli are too noisy at the low frequency range to determine the slope. The 0.1wt% solution containing DMSO also had much lower complex viscosities at both temperatures. At frequencies around 10 rad/s, where the complex viscosities of both solutions were the most stable and farthest apart, the DMSO-

containing solution was two orders of magnitude smaller at 80°C and four orders of magnitude smaller at 20°C.

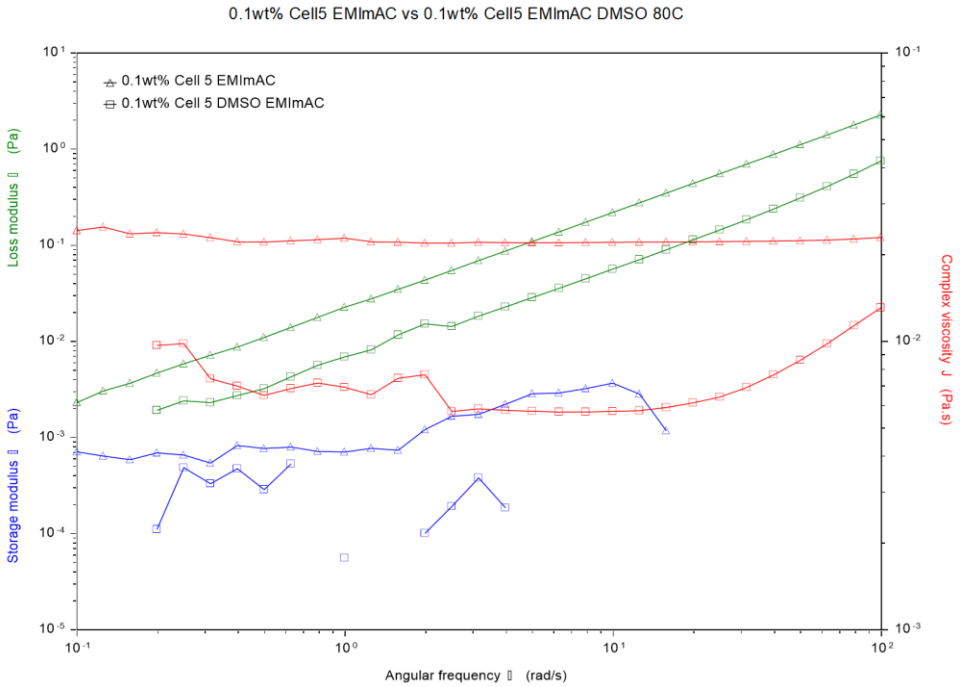

Figure 29: Frequency sweeps of 0.1wt% cellulose in 100% EMImAC (triangles, top) and 50% EMImAC/50% DMSO (squares, bottom) at 80°C

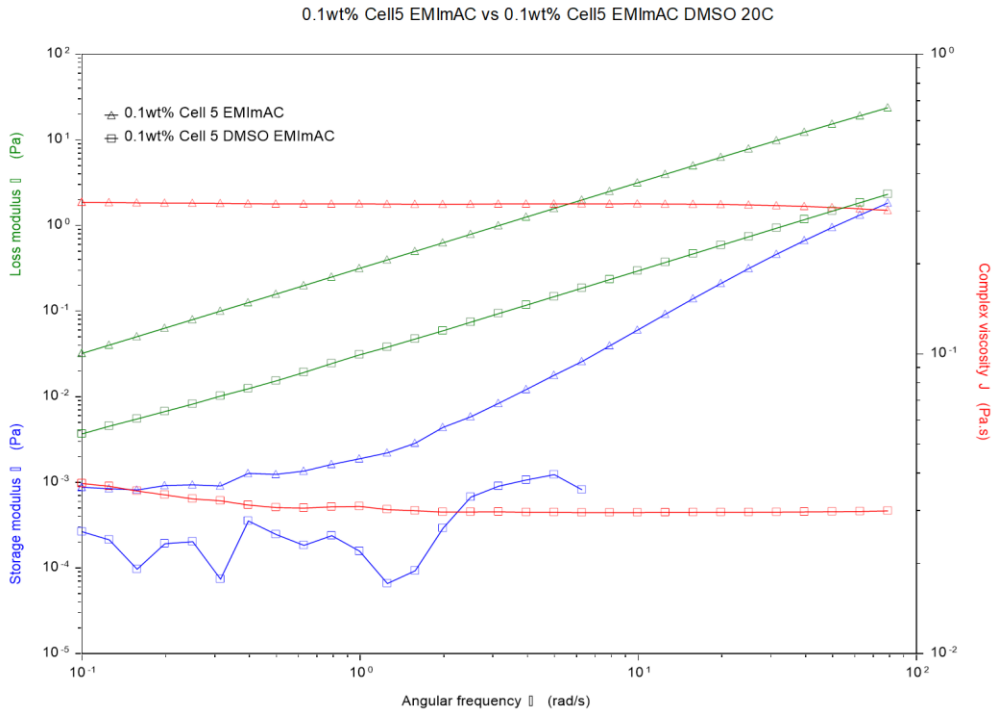

Figure 30: Frequency sweeps of 0.1wt% cellulose in 100% EMImAC (squares, top) and 50% EMImAC/50% DMSO (triangles, bottom) at 80°C

Figures 31 and 32 compare the frequency sweeps of the 0.2wt% cellulose solution in 100% EMImAC and the 0.2wt% cellulose solution in 50% EMImAC/50% DMSO at 80°C and 20°C, respectively. At 80°C, both the sample containing DMSO and the sample without DMSO were characterized as liquid-like due to the loss modulus being larger than the storage modulus. However, as noted in the previous section, 0.2wt% cellulose sample without DMSO does not behave like a liquid and instead appears to act elastically like a solid or gel. The 0.2wt% cellulose sample exhibits a loss modulus greater than the storage modulus at both temperatures, and does not appear to behave elastically. The slopes of the loss moduli of both samples at 80°C but only the DMSO-containing sample at 20°C seem to approach 1, indicating a terminal response, but the slopes of the storage moduli are too noisy at the low frequency range to

determine the slopes, though they also appear to approach 2. The 0.2wt% solution containing DMSO also had a much lower complex viscosity at both temperatures. In the 80°C frequency sweep around 10 rad/s, the DMSO-containing solution was two orders of magnitude smaller than that of the solution without DMSO. The complex viscosities of the solutions could not be accurately compared at 20°C, as the complex viscosity of the 100% EMImAC sample changed with frequency.

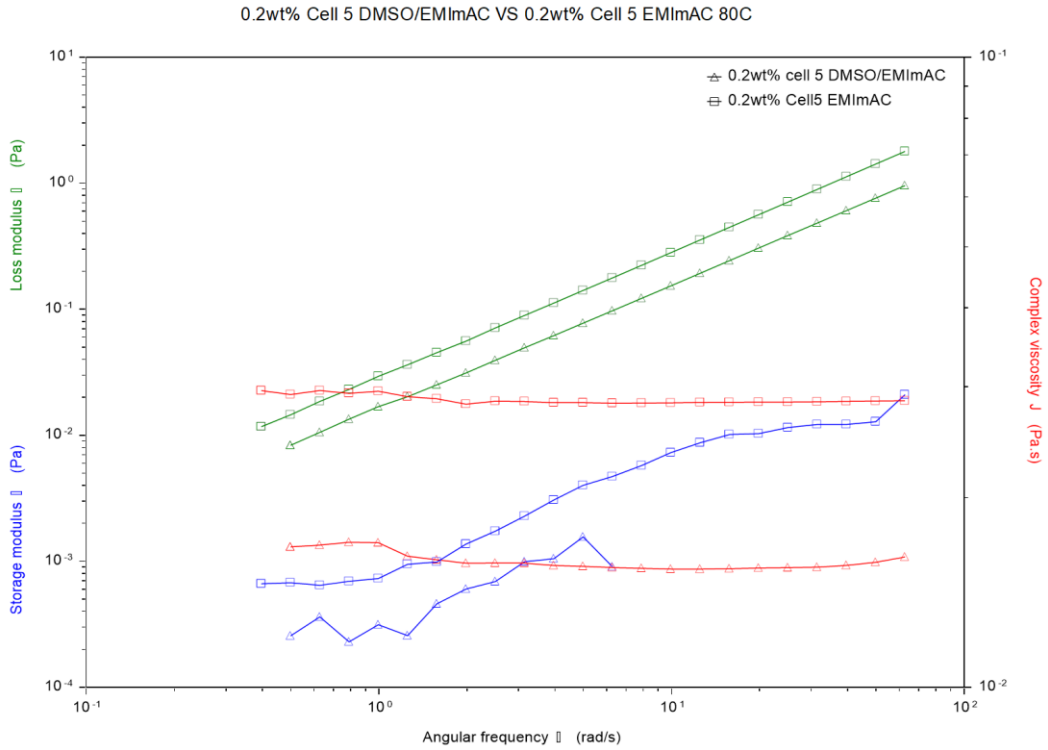

Figure 31: Frequency sweeps of 0.2wt% cellulose in 100% EMImAC (triangles, top) and 50% EMImAC/50% DMSO (squares, bottom) at 80°C

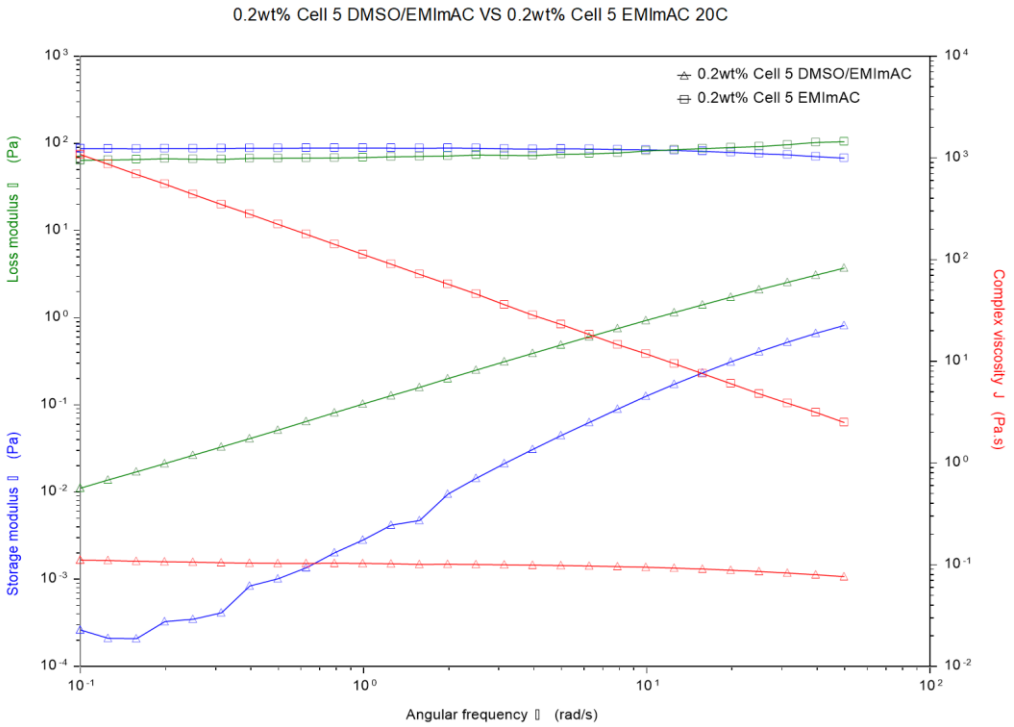

Figure 32: Frequency sweeps of 0.2wt% cellulose in 100% EMImAC (squares, top) and 50% EMImAC/50% DMSO (triangles, bottom) at 20°C

Figures 33 and 34 compare the frequency sweeps of the 0.3wt% cellulose solution in 100% EMImAC with the 0.3wt% cellulose solutions in 50% EMImAC/50% DMSO (prepared either via the 1 vial method or the 3 vial method) at 80°C and 20°C, respectively. Both of the samples containing DMSO and the sample without DMSO behaved as a liquid, indicated by the loss moduli being larger than the storage moduli. All of the samples seem to emulate a terminal response at both temperatures, but the 0.3wt% cellulose sample containing DMSO and prepared via the 3-vial method approached the terminal regime the fastest. Continuing the trend seen at lower concentrations, the 0.3wt% solutions containing DMSO also had much lower complex viscosities at both temperatures. In the 80°C frequency sweep around 10 rad/s, the DMSO-containing solution prepared via 1 vial method was three orders of magnitude smaller than that

of the solution without DMSO, and the DMSO-containing solution prepared via 3 vial method two orders smaller. Unlike the trend seen in smaller concentrations, the complex viscosities of the solutions at 20°C were closer in magnitude than the complex viscosities of the solutions at 80°C.

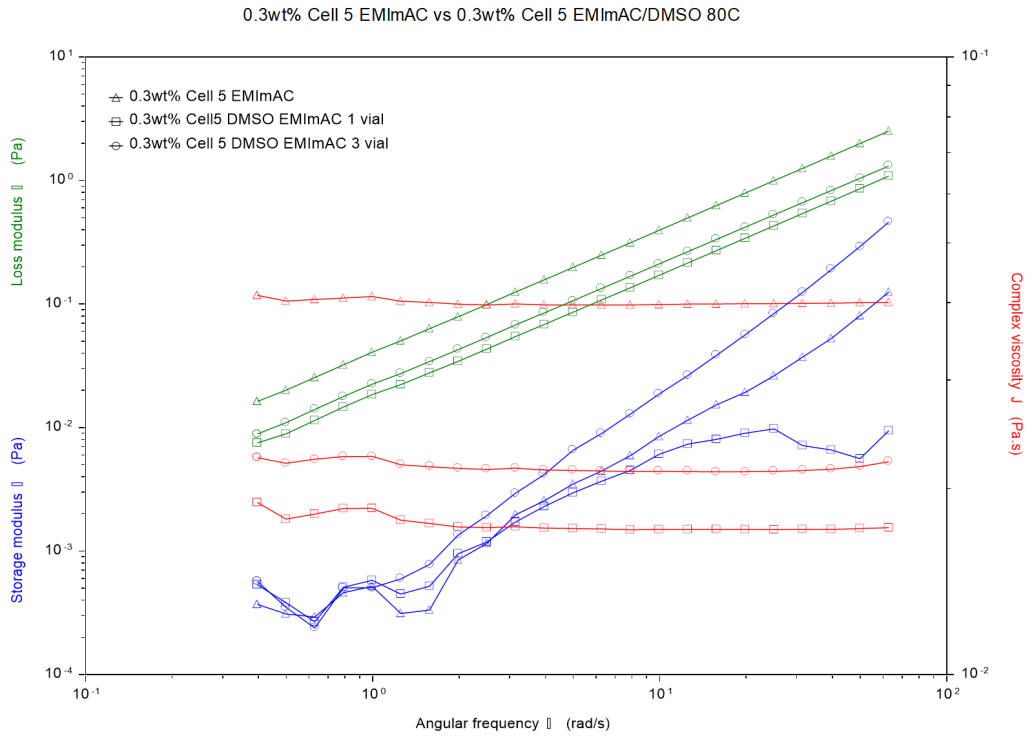

Figure 33: Frequency sweeps of 0.3wt% cellulose in 100% EMImAC, 0.3wt% cellulose in 50% EMImAC/50% DMSO prepared via the 1 vial method, and the 0.3wt% cellulose in 50% EMImAC/50% DMSO prepared via the 3 vial method at 80°C

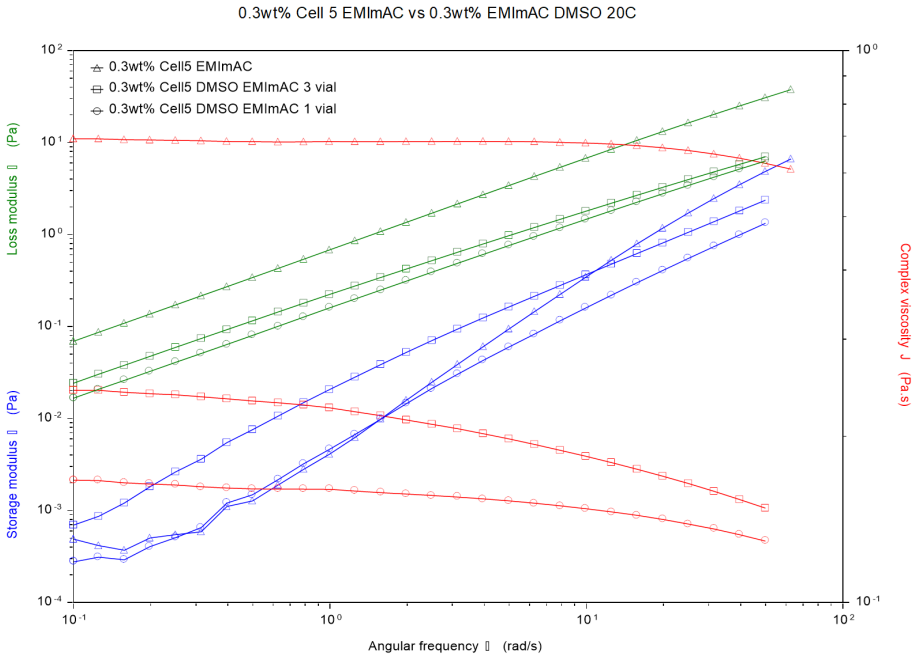

Figure 34: Frequency sweeps of 0.3wt% cellulose in 100% EMImAC, 0.3wt% cellulose in 50% EMImAC/50% DMSO prepared via the 1 vial method, and the 0.3wt% cellulose in 50% EMImAC/50% DMSO prepared via the 3 vial method at 20°C

Chapter 8

Conclusions and Future Study

This thesis has investigated the rheological behaviors of cellulose dissolved in solutions composed of the ionic liquid EMImAC and a cosolvent DMSO. In order to determine the effect DMSO had on the properties of the ionic liquid/cellulose systems, interfacial rheology tests and capillary viscometry experiments were performed with samples containing four different concentrations of cellulose in either 100% EMImAC or a solvent mixture composed of 50% DMSO and 50% EMImAC. The temperature dependence of each set of samples was also investigated by performing each test at 80°C and 20°C.

The intrinsic viscosities of solutions with different concentrations of cellulose was determined using capillary rheometry to measure the relative viscosity of each sample. The inherent and reduced viscosities of the cellulose and EMImAC system were plotted in a Huggins and Kraemer plot for two different temperatures. The Huggins and Kraemer plots were used to calculate the inherent viscosity as well as both the Huggins and the Kraemer coefficients at both 20°C and 80°C. While no Huggins and Kraemer plot was able to be obtained from the cellulose/EMImAC/DMSO system, the relative viscosity of the 0.3wt% cellulose solution containing DMSO was compared to that of the 0.3wt% cellulose solution in 100% EMImAC. It was determined that the addition of DMSO as a cosolvent reduced the relative viscosity of the solution. It was also determined that the strong temperature dependence of the EMImAC/DMSO samples indicated that the solvent quality of the mixture improved with increasing temperature.

The rheological behavior of the cellulose samples in EMImAC and in the EMImAC/DMSO blend were investigated through a series of oscillatory shear experiments. A frequency sweep was performed on each sample at 80°C and 20°C, and the resulting data was

evaluated. By comparing the storage modulus, loss modulus, and complex viscosities of EMImAC and EMImAC/DMSO samples of the same concentration of cellulose at 80°C and 20°C , the effect of the cosolvent was determined. All of the samples of both types of solvent were characterized by a liquid-like response, which was indicated by a loss modulus larger than the storage modulus through the range of frequencies. Additionally, most of the samples appeared to reach the terminal response regime of a viscoelastic liquid at low frequencies. In comparing the complex viscosities of the samples of the same concentration of cellulose with and without DMSO, it was determined that the addition of a cosolvent reduced the viscosity of the system on the order of several magnitudes. The temperature appeared to affect how much the viscosity was reduced, but the trend was not consistent with concentration.

Two methods of sample preparation were similarly investigated in order to determine the best way to prepare consistent, uniform samples of large volumes (12mL). The first method, in which 12mL of the solvent was directly added to the cellulose, was termed the "1 vial method", and the second, in which the 12mL of solvent and cellulose were split into three vials, was termed the "three vial method". Both methods were evaluated using the capillary viscometer and the interfacial rheometer, and it was determined that the "three vial method" should be used in the future due to the higher viscosities of the samples prepared in this manner. The higher viscosities of the samples produced using the three vial method indicate that all of the cellulose was fully and uniformly dissolved.

The results from the investigations into the rheological behavior of cellulose solutions in pure ionic liquid and in solutions containing 50% DMSO support the conclusion that the addition of a cosolvent decreases the viscosity of the cellulose/IL system. Furthermore, it was determined that this effect is temperature-dependent, and that the solvent quality is correlated with higher

temperatures. The results of this study continue the discussion on the use of ionic liquids as cellulose solvents as well as the potential for cosolvents to improve the desirable properties of cellulose solutions, specifically decreased viscosity. The results have broad implications for several applications of cellulose and cellulose solutions, as the processing of the highly attractive biodegradable and biocompatible polymer relies entirely on its dissolution. Decreasing the viscosity of cellulose solutions eliminates one of the major roadblocks in the widespread usage of ionic liquids as solvents. In addition, reducing the viscosity of cellulose solutions may facilitate the production of cellulose-based fibers due to the limitations of fiber-spinning machinery.

Future Study

The next step in this investigation involves continuing the study of the effect of cosolvents on the rheological behavior of cellulose/IL systems. Future experiments should determine how the amount or proportion of DMSO in cellulose/IL solutions changes the viscosity. Moreover, the addition of DMSO should be investigated with higher concentrations of cellulose, as the rheological properties of cellulose solutions change as the cellulose molecules become increasingly associated and entangled. Repeating the experiments with different ionic liquids and different cosolvents would also increase the breadth and depth of information available on the effect of cosolvents on IL/cellulose solutions. Different sources of cellulose with different degrees of polymerization and molecular weight distributions could also be studied in the future. Finally, though rheological measurements using a plate-plate or a cone-and-plate system can be a good indication of whether a solution is spinnable, it is only the beginning of

determining whether a solution can make a fiber. The conditions of the spinneret in each fiber-spinning machine are different and cannot be modeled. Thus, it is a necessary future investigation to actually spin the cellulose/IL and cellulose/cosolvent/IL systems to truly evaluate their potential for producing fibers.

BIBLIOGRAPHY

[1] T. Liebert, "Cellulose Solvents- Remarkable History, Bright Future," in *Cellulose Solvents: For Analysis, Shaping and Chemical Modifiction*, American Chemical Society, 2010, pp. 3-54.

[2] Y. Zhao, X. Liu, J. Wang and S. Zhang, "Insight into the Cosolvent Effect of Cellulose Dissolution in Imidazolium-Based Ionic Liquid Systems," *J. Phys. Chem. B*, vol. 117, no. 30, pp. 9042-9049, 2013.

[3] L. K. Hauru, M. Hummel, K. Nieminen, A. Michud and H. Sixta, "Cellulose Regeneration and Spinnability from Ionic Liquids," *Soft Matter*, vol. 12, pp. 1487-1495, 2016.

[4] T. Heinze, "Cellulose: Structure and Properties," in *Cellulose Chemistry and Properties: Fibers, Nanocelluloses, and Advanced Materials*, vol. 271, O. Rojas, Ed., Springer, Cham., 2015.

[5] P. K. Gupta, S. S. Raghunath, D. V. Prassanna, P. Venkat, V. Shree, C. Chithananthan, S. Choudhary, K. Surender and K. Geetha, "An Update on Overview of Cellulose, Its Structure and Applications," in *Cellulose*, London, IntechOpen, 2019.

[6] H. V. Lee, B. A. Hamid and S. K. Zain, "Conversion of Lignocellulosic Biomass to Nanocellulose: Structure and Chemical Process," *The Scientific World Journal*, vol. 2014, 2014.

[7] K. Matyjaszewski and M. Moller, Eds., "Celluloses and Polyoses/Hemicelluloses," in *Polymer Science: A Comprehensive Review*, vol. 10, Elsevier, 2012.

[8] Y. Lv, J. Wu, J. Zhang and Y. Niu, "Rheological properties of cellulose/ionic liquid/dimethylsulfoxide (DMSO) solutions," *Polymer,* vol. 53, no. 12, pp. 2524-2531, 2012.

[9] F. P. Burns, P. A. Themens and K. Ghandi, "Assessment of phosphonium ionic liquid-dimethylformamide mixtures for dissolution of cellulose," *Composite Interfaces,* vol. 21, no. 1, pp. 59-73, 2014.

[10] E. Gale, R. H. Wirawan, R. L. Silveira and C. S. Pereira, "Directed Discovery of Greener Cosolvents: New Cosolvents for Use in Ionic Liquid Based Organic Electrolyte Solutions for Cellulose Dissolution," *ACS Sustainable Chem. Eng.*, vol. 4, no. 11, pp. 6200-6207, 2016.

[11] I. Bahadur and R. Phadagi, "Ionic Liquids as Environmental Benign Solvents for Cellulose Chemistry: A Review," in *Solvents, Ionic Liquids, and Solvent Effects*, D. Glossman-Mitnik and M. Maciejewska, Eds., London, IntechOpen, 2020, pp. 174-178.

[12] Y. Tomimatsu, H. Suetsuga, Y. Yoshimura and A. Shimizu, "The solubility of cellulose in binary mixtures of ionic liquids and dimethyl sulfoxide: Influence of the anion," *Journal of Molecular Liquids,* vol. 279, pp. 120-126, 2019.

[13] A. Ravve, "Physical Properties and Physical Chemistry of Polymers," in *Principles of Polymer Chemistry*, New York, NY: Springer, 2012, pp. 27-57.

[14] M. Gericke, K. Schlufter, T. Liebert, T. Heinze and T. Budtova, "Rheological Properties of Cellulose/Ionic Liquid Solutions: From Dilute to Concentrated States," *Biomacromolecules,* vol. 10, no. 5, pp. 1188-1194, 2009.

[15] "Polymer Liquids," in *Polymer Physics*, Oxford, Oxford University Press, 2007, pp. 13-14.

[16] N. Weiß, C. H. Schmidt, G. Thielemann and E. Heid, "The physical significance of the Kamlet–Taft π* parameter of ionic liquids," *Phys. Chem. Chem. Phys.*, vol. 23, pp. 1616-1626, 2021.

[17] A. Y. Malkin and A. Isayev, "Viscoelasticity," in *Rheology: Concepts, Methods, and Applications*, Toronto, ChemTec Publishing , 2017, pp. 45-68.

[18] "Rheometry 101: Learning the Basics," AZO Materials, 11 April 2019. [Online]. Available: https://www.azom.com/article.aspx?ArticleID=16985.

[19] "The Molecular Origin of Rheological Properties," in *Polymer Chemistry: Properties and Applications*, Munich, Hanser Publishers, 2006, pp. 107-112.

[20] R. J. Young and P. A. Lovell, "Friction Properties of Polymers in Solution," in *Introduction to Polymers*, Taylor & Francis Group, 2011, pp. 299-303.

[21] D. G. Baird and D. I. Collias, "Viscous Behavior of Polymer Melts," in *Polymer Processing: Principles and Design*, Hoboken, NJ: John Wiley & Sons, 2014, pp. 10-14.

[22] "The Rouse-Bueche Theory," in *Introduction to Polymers*, Taylor & Francis Group, 2011, pp. 393-394.

[23] M. Rubinstein and R. H. Colby, "Unentangled Polymer Dynamics," in *Polymer Physics*, Oxford, Oxford University Press, 2007, pp. 312-314.

[24] S. Sen, J. D. Martin and D. S. Argyropoulos, "Review of Cellulose Non-Derivatizing Solvent Interactions with Emphasis on Activity in Inorganic Molten Salt Hydrates," *ACS Sustainable Chem. Eng.*, vol. 1, no. 8, pp. 858-870, 2013.

[25] M. Isik, H. Sardon and D. Mecerreyes, "Ionic Liquids and Cellulose: Dissolution, Chemical Modification and Preparation of New Cellulosic Materials," *Int. J. Mol. Sci.*, vol. 15, no. 7, pp. 11922-11940, 2014.

[26] A. Xu, Y. Zhang, Y. Zhao and J. Wang, "Cellulose dissolution at ambient temperature: Role of preferential solvation of cations of ionic liquids by a cosolvent," *Carbohydrate Polymers,* vol. 92, no. 1, pp. 540-544, 2013.

[27] J.-M. Andanson, E. Bordes, J. Devemy and F. Leroux, "Understanding the role of co-solvents in the dissolution of cellulose in ionic liquids," *Green Chemistry,* vol. 16, pp. 2528-2538, 2014.

[28] O. A. El Seoud and T. A. Bioni, "Understanding cellulose dissolution in ionic liquid-dimethyl sulfoxide binary mixtures: Quantification of the relative importance of hydrogen bonding and hydrophobic interactions," *Journal of Molecular Liquids,* vol. 322, 2021.

[29] A. Xu, L. Cao, B. Wang and J. Ma, "Dissolution Behavior of Cellulose in IL + DMSO Solvent: Effect of Alkyl Length in Imidazolium Cation on Cellulose Dissolution," *Advances in Materials Science and Engineering,* vol. 2015, 2015.

[30] N. Utomo, Rheology of Native Cellulose Solutions in Ionic Liquids, Universtiy Park, PA: The Pennsylvania State University, 2019.

[31] B. Nazari, N. W. Utomo and R. H. Colby, "The Effect of Water on Rheology of Native Cellulose/Ionic Liquids Solutions," *Biomacromolecules,* vol. 18, no. 9, pp. 2849-2857, 2017.

[32] B. Azimi, H. Maleki and V. Gigante, "Cellulose-based fiber spinning processes using ionic liquids," *Cellulose,* 2022.

[33] S. Koltzenburg, M. Maskos and O. Nuyken, "The Basics of Plastics Processing," in *Polymer Chemistry*, 2017, pp. 439-476.

[34] Y. Liu, Y. Nie and P. Fengjiao, "Study on ionic liquid/cellulose/coagulator phase diagram and itsapplication in green spinning process," *Journal of Molecular Liquids,* vol. 289, no. 2019, 2019.

[35] L. Hardelin, L. Thunberg and E. Perzon, "Electrospinning of cellulose nanofibers from ionic liquids: The effect of different cosolvents," *Journal of Applied Polymer Science,* vol. 125, no. 3, pp. 1901-1909, 2012.

[36] S.-L. Quan, S.-G. Kang and I.-J. Chin, "Characterization of cellulose fibers electrospun using ionic liquid," *Cellulose,* vol. 17, pp. 223-230, 2009.

[37] N. A. Nguyen, K. Kim and C. C. Bowland, "A fundamental understanding of whole biomassdissolution in ionic liquid for regeneration offiberby solution-spinning," *Green Chemistry,* vol. 21, 2019.

[38] S. Elsayed, M. Hummel and D. Sawada, "Superbase-based protic ionic liquids for cellulose filament spinning," *Cellulose,* vol. 28, pp. 533-547, 2021.

[39] L. K. Hauru, M. Hummel and A. Michud, "Dry jet-wet spinning of strong cellulose filaments from ionic liquid solution," *Cellulose,* vol. 21, pp. 4471-4481, 2014.

[40] IOLITEC, "1-Ethyl-3-methylimidazolium acetate," 2019. [Online]. Available: https://iolitec.de/sites/iolitec.de/files/2019-08/TDS%20IL-0189%20EMIM%20OAc.pdf.

[41] Sigma-Aldrich, "Dimethyl Sulfoxide anhydrous, >99.9%," 2010. [Online]. Available: https://www.sigmaaldrich.com/specification-sheets/634/230/276855-BULK_____SIAL_____.pdf.

[42] R. Wattana, "Rheology of Natural Polysaccharides in Ionic Liquids," *Honors Thesis,* 2020.

ACADEMIC VITA

Victoria Belka

vlb5221@psu.edu | victoriabelka@gmail.com

EDUCATION

The Pennsylvania State University State College, PA 16801
Bachelor of Science in Materials Science and Engineering
Schreyer Honors College, College of Earth and Mineral Sciences
Thesis Title: *Rheology of Native Cellulose in Ionic Liquid/DMSO Solutions*
Thesis Supervisor: Ralph Colby, Ph.D.

PROFESSIONAL AND RESEARCH EXPERIENCE

Undergraduate Researcher *Fall 2019-Present*
Department of Materials Science and Engineering, Penn State University
Assisted in research regarding the extraction and study of native cellulose in ionic liquid systems

Camp Counselor *May-August 2019*
Engineering for Kids
Taught children about various fields of engineering through hands-on crafts and activities

AWARDS

Dean's List *Fall 2018-Present*

University Park 4 Year Provost Award *Fall 2018- Present*

Gerald Bayles Memorial Scholarship *Fall 2021-Spring 2022*

C. Philip Cook, Jr. Memorial Scholarship *Fall 2019-Spring 2020*

Norris B. McFarlane Scholarship *Fall 2018-Spring 2019*

2018 EMS Outstanding Research Potential Award *Spring 2018*

SKILLS

Laboratory Equipment: Discovery Hybrid Rheometer 3, Cannon Mini-Automated Viscometer

Engineering Software: MATLAB, R studio

Office Software: Microsoft Office, Adobe Photoshop and Premiere Pro